and A. Wyttenbach, Phys. Rev. 134, B1262 (1964).
[63]F. S. Rowland and R. L. Wolfgang, Phys. Rev. 110, 175 (1958).
[64]P. Boerseling, G. M. Raisbeck, and T. D. Thomas, unpublished.
[65]R. D. Edge, C. W. Darden, W. F. Lankford, and H. D. Orr, III, Bull. Am. Phys. Soc. 13, 1445 (1968).
[66]N. A. Perfilov, O. V. Lozhkin, and V. P. Shamov, Usp. Fiz. Nauk 60, 3 (1960) [transl.: Soviet Phys.–Usp. 3, 1 (1960).
[67]N. A. Perfilov, O. V. Lozhkin, and V. I. Ostroumov, *Yadernye Reakstii pod deistviem chastits vysokekh energii* (Nuclear Reactions Induced by High-Energy Particles) (Academy of Science USSR, Moscow, 1962).
[68]M. Lefort, Ann. Phys. (Paris) 9, 249 (1964).
[69]E. Makowska, J. Sieminska, M. Soltan, J. Suchorzewska, and S. J. St. Lorant, Nucl. Phys. 79, 449 (1966).
[70]V. Weisskopf, Phys. Rev. 52, 295 (1937); K. J. LeCouteur, Proc. Phys. Soc. (London) A63, 259 (1950).
[71]P. A. Gorichev and I. I. P'yanov, Yadern. Fiz. 2, 97 (1965) [transl.: Soviet J. Nucl. Phys. 2, 68 (1966)].
[72]T. Miyazima, K. Nakamura, and Y. Futami, Progr. Theoret. Phys. (Kyoto) Suppl. 34, 621 (1965).
[73]E. Bagge, Ann. Physik 33, 389 (1938); Physik Zeit. 44, 461 (1942).
[74]R. DaSilveira, Phys. Letters 9, 252 (1964).
[75]N. Metropolis, R. Bivens, M. Storm, A. Turkevich, M. M. Miller, and G. Friedlander, Phys. Rev. 110, 185 (1958); 110, 204 (1958).
[76]I. Dostrovsky, Z. Fraenkel, and G. Friedlander, Phys. Rev. 116, 683 (1959).
[77]G. D. Harp, J. M. Miller, and B. J. Berne, Phys. Rev. 165, 1166 (1968).
[78]J. Hudis, in *Nuclear Chemistry*, edited by L. Yaffe, (Academic, New York, 1968), Vol. 1, p. 169.

PHYSICAL REVIEW C VOLUME 4, NUMBER 5 NOVEMBER 1971

Study of the (d, p) Reaction on ^{28}Si, ^{32}S, and ^{36}Ar at $E_d = 18.00$ MeV*

M. C. Mermaz,† C. A. Whitten, Jr.,‡ J. W. Champlin, A. J. Howard,§ and D. A. Bromley
Wright Nuclear Structure Laboratory, Yale University, New Haven, Connecticut 06520
(Received 22 July 1971)

The reactions ^{28}Si$(d,p)^{29}$Si, ^{32}S$(d,p)^{33}$S, and ^{36}Ar$(d,p)^{37}$Ar were studied at an incident deuteron energy of 18.00 MeV. Some ^{28}Si$(d,p)^{29}$Si data were also obtained at an incident deuteron energy of 21.00 MeV. Angular distributions were obtained for proton groups leading to states in the residual nuclei ^{29}Si, ^{33}S, and ^{37}Ar with excitation energies up to approximately 8 MeV. With the use of distorted-wave Born-approximation (DWBA) analyses, spectroscopic factors were obtained for all (d,p) transitions which displayed direct-reaction characteristics. J dependence was observed in $l=2$ $(1d)$ and $l=1$ $(2p)$ (d,p) transitions for $E_d=18.00$ MeV. The spectroscopic factors obtained in this experimental study are compared with the predictions of current theoretical models which treat nuclei in the upper s-d shell.

I. INTRODUCTION

This study of the (d, p) neutron stripping reaction in the upper half of the s-d shell is the third and final paper in a series dealing with experimental studies of deuteron-induced reactions on the even-even, $T=0$ target nuclei ^{28}Si, ^{32}S, and ^{36}Ar. The first paper[1] dealt with 18.00-MeV elastic and inelastic deuteron scattering on these three target nuclei; in the second paper[2] experimental data on the (d, t) neutron-pickup reaction obtained at 21.00 MeV were presented and discussed.

The original impetus for these experimental studies was the suggestion by Ripka[3] – which he directed specifically to ^{28}Si – that a combination of particle-pickup and stripping reactions on a given target nucleus could be used to study changes in the equilibrium shape of the nucleus as particles were added or subtracted. For example, if the low-lying levels of ^{27}Si have a very different equilibrium shape than that of the ground state of ^{28}Si, then the ^{28}Si$(d, t)^{27}$Si neutron-pickup transitions to these levels should be noticeably inhibited. A further impetus for the ^{28}Si, ^{32}S, and ^{36}Ar (d, t) and (d, p) experimental studies was the procurement of accurate experimental spectroscopic information with which current theoretical-model predictions could be compared. Recently a group at the Oak Ridge National Laboratory[4] has performed an extensive set of shell-model calculations for nuclei in the s-d shell ($16< A< 40$). In the upper s-d shell ($A>28$) these calculations consider a shell-model basis which includes holes in the $1d_{5/2}$ shell. Thus they predict $l_n=2$, $1d_{5/2}$ neutron-pickup and stripping spectroscopic factors, as well as $l_n=2$, $1d_{3/2}$ and $l_n=0$, $2s_{1/2}$ spectroscopic factors. In Sec. V we compare the predictions of the Oak Ridge calculations with our experimental (d, p) spectroscopic factors.

Many experimental studies have previously been reported on the ^{28}Si, ^{32}S, and ^{36}Ar (d, p) reactions.[5] However, very few of these experiments studied

(d, p) transitions to states spanning a broad range of excitation energies (0 to 7.5 MeV) in the residual nuclei and extracted (d, p) spectroscopic factors from the experimental data using the distorted-wave Born-approximation (DWBA) theory of the (d, p) reaction. Also, with three exceptions – the 15.0-MeV ^{28}Si(d, p) experiments of Blair and Quisenberry[6] and of Betigeri *et al.*,[7] and the 15.0-MeV ^{36}Ar(d, p) experiment of Rosner and Schneid[8] – all of the reported (d, p) experiments on ^{28}Si, ^{32}S, and ^{36}Ar were performed with incident deuteron energies less than 12.0 MeV. The experimental results presented in this paper on the ^{28}Si, ^{32}S, and ^{36}Ar (d, p) reactions were obtained at a deuteron bombarding energy of 18.00 MeV. At this higher deuteron bombarding energy it was expected that the specifically direct-reaction component of a given (d, p) transition would be enhanced over the compound-nuclear component of this transition. The large increase in the number of possible exit channels with the increase in the incident deuteron energy acts to decrease the compound-nuclear component of any given (d, p) transition, while the direct-reaction component might be expected to remain roughly unchanged in magnitude. In addition to the specific spectroscopic information extracted from the data presented herein, the present (d, p) experiments were intended to provide a general survey of (d, p) angular distributions in the mass region $A \simeq 30$ at these higher deuteron energies.

The experimental setup and procedure used in this experiment are described in Sec. II, while the DWBA analysis is discussed in Sec. III. Section IV presents the experimental results together with the DWBA fits to the experimental (d, p) angular distributions. In this section the extracted (d, p) spectroscopic factors are also presented. In Sec. V the predictions of various theoretical models are compared with the experimental results.

II. EXPERIMENTAL SETUP AND PROCEDURE

The (d, p) experiments reported herein were performed in a 76-cm ORTEC scattering chamber using 18.00- and 21.00-MeV deuteron beams from the Yale MP tandem Van de Graaff accelerator. Typical deuteron beam intensities varied from $\simeq$5 nA at the most forward angle studied ($\theta_{lab} = 10°$), to 500–750 nA at backward angles ($\theta_{lab} > 70°$). In the ^{32}S(d, p) and ^{36}Ar(d, p) experiments, which were performed at 18.00 MeV, a ΔE-E telescope of silicon surface-barrier detectors, standard electronics, and a Landis-Goulding particle identifier of the $[(E + \Delta E)^{1.73} - E^{1.73}]$ type[9] identified and energy analyzed the proton groups of interest.[10] The ΔE detector was 1500 μ in thickness while the E detector was 2000 μ thick. The proton spectra were stored in a standard 1024-channel analyzer. In the ^{28}Si(d, p) experiment at 18.00 MeV, a 1200-μ ΔE and 2000-μ E detector telescope was used with the simple logic requirement that there be a pulse in both the ΔE and E detectors. Unfortunately, at forward angles, elastic deuteron groups from the target compounds silicon and oxygen, as well as from ubiquitous tantalum, carbon, and hydrogen target contaminants penetrated through the ΔE detector and triggered the E-detector logic. At the forward angles this meant that the ^{28}Si(d, p) transitions to levels in ^{29}Si between excitation energies of 5.5 and 7.2 MeV were generally masked by the strong elastic deuteron groups. Data were obtained for these transitions from a ^{28}Si(d, p) run at $E_d = 21.00$ MeV. Here we used the same detector telescope and electronic system as in the ^{32}S(d, p) and ^{36}Ar(d, p) experiments. In order to reduce the detector noise level, the detector telescope was cooled to a temperature of ~0°C by a thermoelectric cooler connected to the telescope mount. The front face of the ΔE detector was covered with a 0.64-μ-thick nickel foil to prevent condensation of oil vapor on the face of the cooled detector. A horseshoe magnet was placed in front of the detector telescope to sweep away low-energy knockout electrons from the target. The total energy resolution in the ^{28}Si, ^{32}S, and ^{36}Ar (d, p) experiments was $\simeq$60 keV.

In the ^{28}Si(d, p) experiments a self-supported foil of natural silicon (^{28}Si 92.3% abundant) oxide was used. This foil was a mixture of the chemical forms SiO and SiO_2 and was approximately 250 μg/cm^2 thick. In the ^{32}S(d, p) and ^{36}Ar(d, p) experiments a gas-cell target was used. This gas cell was 2.54 cm in diameter; a 2.54-μ-thick Havar[11] window extended around much of the cell allowing a wide range of observation angles. The interaction volume in the gas cell was defined by a two-slit collimation system in front of the detector telescope. The front slit had a vertical aperture 0.159 cm wide and was located 5 cm from the center of the gas cell; the back slit had a circular aperture 0.318 cm in diameter and was positioned 21 cm from the center of the gas cell. The angular resolution of this collimation system was about 0.6°.

The sulfur target was H_2S gas of natural isotopic composition (^{32}S 95.06% abundant) and was obtained from a commercial source. The ^{36}Ar gas had greater than 98% isotopic and elemental purities, and was separated by the Yale Isotope Separation group. The gas pressures used in these experiments were approximately 200 Torr. In all of the (d, p) experiments the target condition was monitored by an additional surface-barrier detector

which detected elastic scattering events.

For the ^{28}Si(d, p) experiment at 18.00 MeV, absolute cross sections were determined by normalizing the ^{28}Si(d, p) yields to the yields for the elastic scattering of 4.00-MeV α particles on silicon. The 4.00-MeV α-scattering experiment was carried out under the same conditions of target position and detector geometry as the 18.00-MeV ^{28}Si(d, p) experiment. The α elastic scattering angular distribution at 4.00 MeV was found to obey the Rutherford scattering law out to lab angles of at least 90°. Thus we were able to obtain absolute ^{28}Si(d, p) cross sections directly from the known Rutherford scattering cross sections. This comparison method for determining absolute cross sections was especially valuable in the case of our silicon oxide target, since the target's exact composition in terms of SiO and SiO_2 was not known. For the 18.00-MeV ^{28}Si(d, p) data a conservative estimate of the error in the experimental absolute cross sections is ±10%, excluding counting statistics.

In the ^{32}S(d, p) and ^{36}Ar(d, p) experiments at 18.00 MeV, absolute cross sections were obtained from a standard formula[12] which depends on the geometry of the two-slit collimation system and the density of the gas in the gas cell. The gas density was measured by determining the gas pressure and the temperature of the gas-cell housing. However, local heating of the gas by the deuteron beam raises the local temperature of the gas and thus lowers its density. Therefore, the target gas density is a function of the beam current. In the case of the ^{36}Ar(d, p) experiment we were able to estimate this effect quite accurately by using the monitor detector and plotting the yield of elastic deuterons per μC of beam versus the beam current in nA. The resultant curve could then be extrapolated to zero beam current and no local heating effect. With the H_2S gas target, in addition to the local heating of the gas by the beam, the H_2S gas itself was cracked, mainly at the entrance and exit foils of the gas cell, so that the H_2S gas density decreased monotonically as a function of time. This cracking of the H_2S gas was checked by mass spectrometer analyses on the gas sample before and after a series of runs. After a series of runs which represented about 2500 μC of integrated charge with beam currents between 10 and 300 nA, the amount of hydrogen gas in the H_2S sample had increased by a factor of about 30. This monotonic decrease in the H_2S gas density because of cracking made it more difficult to estimate the effect of local heating. Conservative estimates of the errors in the absolute cross sections for the ^{32}S(d, p) and ^{36}Ar(d, p) experiments would be ±15 and ±8%, respectively, excluding counting statistics. In all three experiments – ^{28}Si(d, p), ^{32}S(d, p), and ^{36}Ar(d, p) – the accuracy of the relative cross sections from angle to angle is mainly determined by the counting statistics, in general much less than 10%, since the experimental yields are normalized to the yield of the detector which continuously monitored the target condition.

III. DWBA ANALYSIS

Zero-range, local DWBA calculations using the Oak Ridge computer program JULIE[13,14] were performed in order to extract spectroscopic information from the experimental (d, p) angular distributions. The deuteron and proton optical-model parameters used in these calculations are listed in Table I. The deuteron optical-model parameters are very similar to those used in the optical-model analysis of 18.00-MeV deuteron elastic scattering on silicon.[1] The proton optical-model parameters were taken from the work of Perey.[15] The wave function of the neutron stripped in the (d, p) reaction was calculated from a potential well of the Woods-Saxon shape. The radius parameter of the well, r_n, was 1.25 F; the diffusivity parameter, a_n, was 0.65 F; and a spin-orbit strength, λ, equal to 25.0 was used. The magnitude of the bound-neutron potential was varied to reproduce the neutron binding energy $[B(n) = Q(d, p) + 2.225$ MeV$]$.

Spectroscopic factors were calculated from the relation

$$\sigma(\text{expt}) = 1.58(2J+1)S\sigma(\text{DWBA}),$$

where J is the spin of the level reached by the (d, p) transition. The factor 1.58 rather than 1.50

TABLE I. Optical-model parameters used in the DWBA analyses.

Particle	V_0 (MeV)	W' [a] (MeV)	V_{so} (MeV)	r_0 (F)	r_{0c} (F)	r'_0 (F)	a (F)	a' (F)	Reference
Deuteron	124.7	89.7	···	0.919	1.30	1.422	0.943	0.541	1
Proton	44.0	38.5	8.5	1.25	1.25	1.25	0.65	0.47	15

[a] In the DWBA computer program JULIE the surface-peaked imaginary potential in the optical-model potential is given by $W(r) = iW'(d/dx')(1+e^{x'})^{-1}$; $x' = (r - r'_0 A^{1/3})/a'$. $W(r)$ is also often defined by $W(r) = i\,4a'\,W_D\,(d/dr)(1+e^{x'})^{-1}$. Thus $W' = 4W_D$.

has been suggested by Goldfarb[16] to account for the effect of the deuteron D state. In taking the ratio of σ(expt) and σ(DWBA) to determine the spectroscopic factor we weighted most heavily those points around the forward maximum of a given (d, p) transition.

The DWBA calculations for each (d, p) transition were carried out using both no radial cutoff ($R_C = 0$) and a radial cutoff at the nuclear surface ($R_C \cong 4.0$ F). The $R_C = 0$ and $R_C = 4.0$ F DWBA curves gave about equally good fits to the experimental data; and for a given (d, p) transition the spectroscopic factors obtained from these two curves differed by less than 25%. All the DWBA curves and spectroscopic factors presented in Sec. IV were obtained from DWBA calculations with $R_C = 0$.

IV. EXPERIMENTAL RESULTS

A. General Comments

The final nuclei – ^{29}Si, ^{33}S, and ^{37}Ar – reached in the present (d, p) study have been previously studied by many experimenters using a great variety of techniques. This work has been summarized in the $Z = 11$–21 compilation of Endt and Van der Leun.[5] Unless otherwise specified the excitation energies and spin and parity assignments used in the present paper are taken from this compilation.

In the analysis of the experimental data we have tried to study (d, p) transitions to highly excited levels in ^{29}Si, ^{33}S, and ^{37}Ar. Taking into account our 60-keV experimental resolution and the known energy-level density in these nuclei,[5] it is clear that not all of the experimental proton groups will represent (d, p) transitions to single, well-resolved levels in the final nucleus. However, we have analyzed most of the proton groups which have an appreciable cross section at the forward angles (10 to 30°). Most of the strong (d, p) transitions to states between about 3.5- and 8.0-MeV excitation energy are expected to represent $l = 1$ and $l = 3$ neutron stripping into the $1f$-$2p$ shell. Now for an $l = 1$ (d, p) transition where $(2J + 1)S = 1.0$, the peak experimental cross section would be approximately 15 mb/sr. This favorable ratio allows us to determine $l = 1$ (d, p) transitions with values of $(2J + 1)S > 0.1$. For the case of $l = 3$ (d, p) transitions, a peak cross section of approximately 3 mb/sr represents a transition for which $(2J + 1)S = 1.0$. Thus this experiment is approximately five times more sensitive for $l = 1$ (d, p) transitions than for $l = 3$ (d, p) transitions.

B. Reaction ^{28}Si$(d, p)^{29}$Si at 18.00 MeV

Figure 1 presents the experimental proton and elastic deuteron spectrum at a lab angle of 45° obtained from the bombardment of a silicon oxide target with 18.00-MeV deuterons. The origin of the elastic deuteron groups was discussed in Sec. II. At forward angles these elastic deuteron groups masked many ^{28}Si(d, p) transitions corresponding to excitation energies in ^{29}Si between about 5.2 and 7.2 MeV. In Sec. IV C ^{28}Si$(d, p)^{29}$Si data are presented which cover this range of excitation energy in ^{29}Si. Aside from the elastic deuteron groups, the experimental spectrum also contains proton groups from the reactions ^{16}O$(d, p)^{17}$O and ^{12}C$(d, p)^{13}$C, reflecting use of an oxide target and a carbon contamination in this target. In this section data are presented for ^{28}Si(d, p) transitions leading to levels in ^{29}Si between 0 and 5.0 MeV and between 6.5 and 8.6 MeV. Figures 2–4 display the

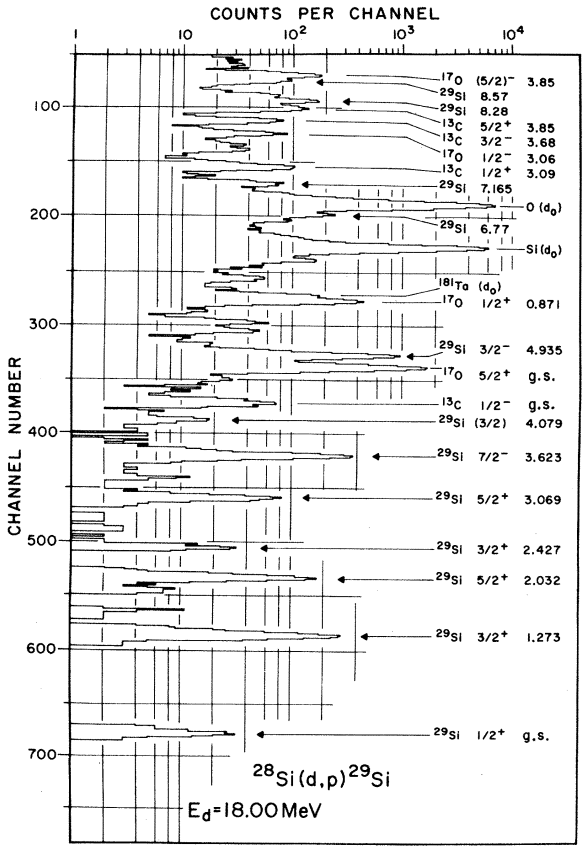

FIG. 1. Experimental proton and elastic deuteron spectrum at $\theta_{lab} = 45°$ from the bombardment of 18.00-MeV deuterons on a silicon oxide target (^{28}Si 92.28%, ^{29}Si 4.67%, and ^{30}Si 3.05%). As is discussed in Sec. II, the elastic deuteron groups originated from the particular detector telescope and electronic logic used in this experiment. The majority of the experimental (d,p) transitions correspond to the reaction ^{28}Si$(d,p)^{29}$Si ($Q_m = +6.251$ MeV). However, strong ^{16}O$(d,p)^{17}$O transitions from the oxide target are also observed, as well as weaker ^{12}C$(d,p)^{13}$C transitions from a carbon contamination in the target.

experimental data and the DWBA fits to these data, while Table II presents the spectroscopic information.

Figure 2 presents the (d, p) angular distributions to the known $\frac{1}{2}^+$, $\frac{3}{2}^+$, and $\frac{5}{2}^+$ levels in ^{29}Si below 3.1 MeV.[5] The ^{28}Si(d, p) angular distribution to the $\frac{1}{2}^+$ ground state is well fitted by an $l=0$, $2s_{1/2}$ DWBA curve. The (d, p) transitions to the $\frac{3}{2}^+$ 1.273-MeV, the $\frac{5}{2}^+$ 2.032-MeV, and $\frac{5}{2}^+$ 3.069-MeV levels all show distinctive $l=2$ (d, p) stripping patterns, while the (d, p) angular distribution to the $\frac{3}{2}^+$ 2.427-MeV level does not show evidence for forward-angle stripping. The forward-angle cross sections for the $\frac{3}{2}^+$ 2.427-MeV level allow a fairly low upper limit to be placed on the possible $l=2$ stripping strength to this level (Table II). Figure 3 presents the strong ^{28}Si(d, p) transitions to the $\frac{7}{2}^-$ 3.623-MeV and $\frac{3}{2}^-$ 4.935-MeV levels of ^{29}Si. The $(\frac{3}{2})$ 4.079-MeV level in ^{29}Si is excited quite weakly in these ^{28}Si(d, p) data. The spectroscopic factors obtained from these ^{28}Si(d, p) data at $E_d = 18.00$ MeV for $E_x(^{29}\text{Si}) < 5.0$ MeV agree reasonably well with those obtained by Betigeri *et al.*[7] from $E_d = 15$-MeV ^{28}Si$(d, p)^{29}$Si data.

Many ^{29}Si levels have been previously observed with excitation energies between 6.5 and 9.0 MeV[5]; but no l assignments have been reported for these levels in the ^{28}Si(d, p) reaction. In the present experiment fairly complete forward-angle (d, p) angular distributions were obtained for four ^{29}Si levels at 6.77 ± 0.02, 7.165 ± 0.020, 8.28 ± 0.02, and 8.57 ± 0.02 MeV. Some data were also obtained for a ^{29}Si level at 6.90 ± 0.02 MeV. The excitation energies for these five levels were obtained from a proton energy calibration curve which used the experimental positions of the ^{16}O$(d, p)^{17}$O and ^{12}C$(d, p)^{13}$C proton groups (see Fig. 1). With the possible exception of the 6.77-MeV level these levels can be almost certainly identified with ^{29}Si, since their corresponding proton groups shift kinematically as $A \sim 29$ and their spectroscopic strengths would be huge (see Table II) if they were ^{29}Si(d, p) or ^{30}Si(d, p) transitions. The experimental width for all five proton groups is no wider than that expected for a single level.

The (d, p) angular distribution for the 6.77-MeV level in ^{29}Si (Fig. 4) is quite well fitted by an $l=4$, $1g_{9/2}$ DWBA curve. The $l=4$ spectroscopic strength for this transition represents 6% of the total $1g_{9/2}$ single-particle strength (Table II). Due to the lack of forward-angle points (Fig. 4), the stripping characteristics of the (d, p) transition to the 6.90-MeV level in ^{29}Si could not be determined.

Figure 4 also presents the (d, p) angular distributions to the ^{29}Si levels at 7.165, 8.28, and 8.57 MeV. These angular distributions have been fitted

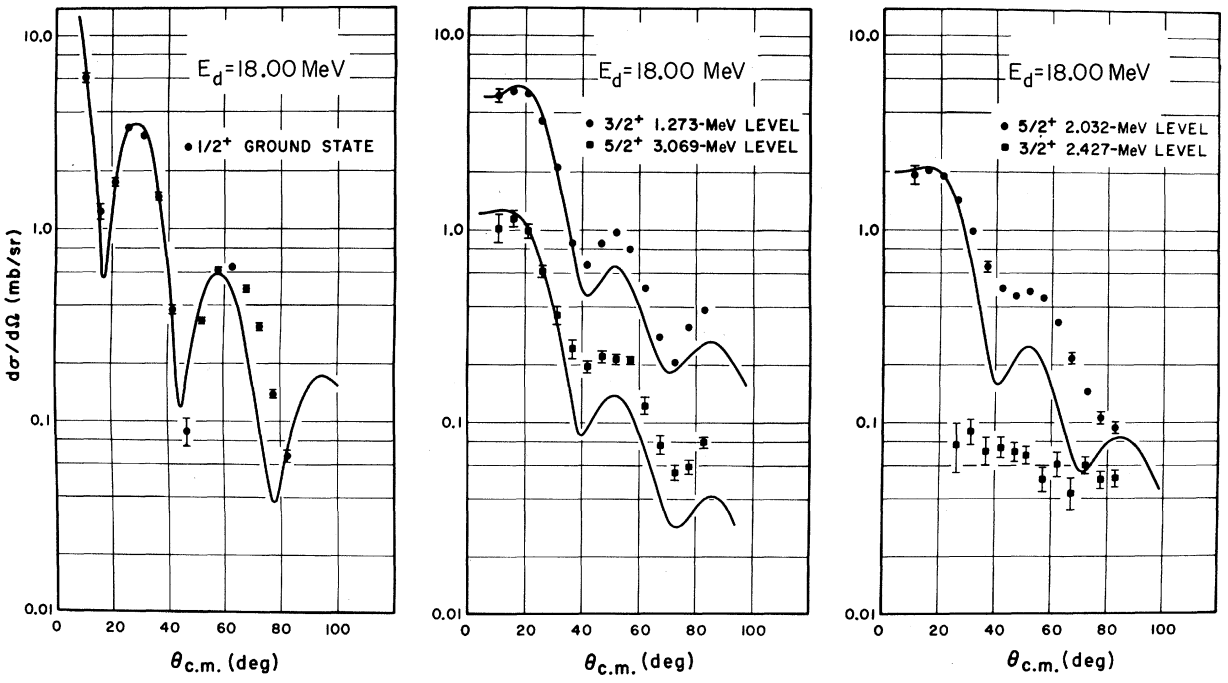

FIG. 2. ^{28}Si$(d,p)^{29}$Si angular distributions for the $\frac{1}{2}^+$ ground state, the $\frac{3}{2}^+$ 1.273-, the $\frac{5}{2}^+$ 3.069-, the $\frac{5}{2}^+$ 2.032-, and the $\frac{3}{2}^+$ 2.427-MeV levels. The solid curves represent the appropriately labeled DWBA fits for the first four of these transitions; the (d,p) transition to the 2.427-MeV level does not display discernible forward-angle stripping characteristics.

with both $l=3$, $1f$ and $l=2$, $1d$ DWBA curves, and the corresponding spectroscopic strengths are presented in Table II. At these excitation energies it would be more likely to find $1f$ rather than $1d$ spectroscopic strength; but the $l=2$ curve provides a better fit for the 7.165-MeV level and also possibly for the 8.57-MeV level. The extracted $l=2$ spectroscopic strength $[(2J+1)S \cong 0.25]$ to the 7.165- and 8.57-MeV levels does not eliminate the possibility that one or both of these transitions are indeed $l=2$. Since the (d, p) angular distribution for the 8.28-MeV level is better fitted by the $l=3$ DWBA curve and the extracted $l=2$ spectroscopic strength of 1.4 would be larger than expected for a level at this excitation energy, it is fairly certain that the (d, p) transition to the 8.28-MeV level is $l=3$. Since the 8.57-MeV level is neutron unbound by about 90 keV, the DWBA curves for this level were obtained by extrapolation from the bound levels.

C. Reaction ^{28}Si$(d, p)^{29}$Si at 21.00 MeV

In this section we present 21.00-MeV data for the ^{28}Si$(d, p)^{29}$Si transitions which were masked by elastic deuteron groups in the 18.00-MeV data discussed in Sec. IV B. Only strong (d, p) transitions to levels in ^{29}Si with excitation energies between 5.5 and 6.5 MeV were investigated in the 21.00-MeV experiment. Three levels in this range of excitation energies were excited strongly; the experimental angular distributions to these levels are presented in Fig. 5 along with DWBA fits which use the optical-model parameters tabulated in Table I. In the 21.00-MeV data the thickness of the silicon oxide was not determined, so that the spectroscopic factors for the transitions to the 5.944-, 6.195-, and 6.382-MeV levels in ^{29}Si were determined by a normalization procedure. At 21.00 MeV the DWBA curves for the strong transitions to the $\frac{7}{2}^-$ 3.623-MeV and $\frac{3}{2}^-$ 4.935-MeV levels

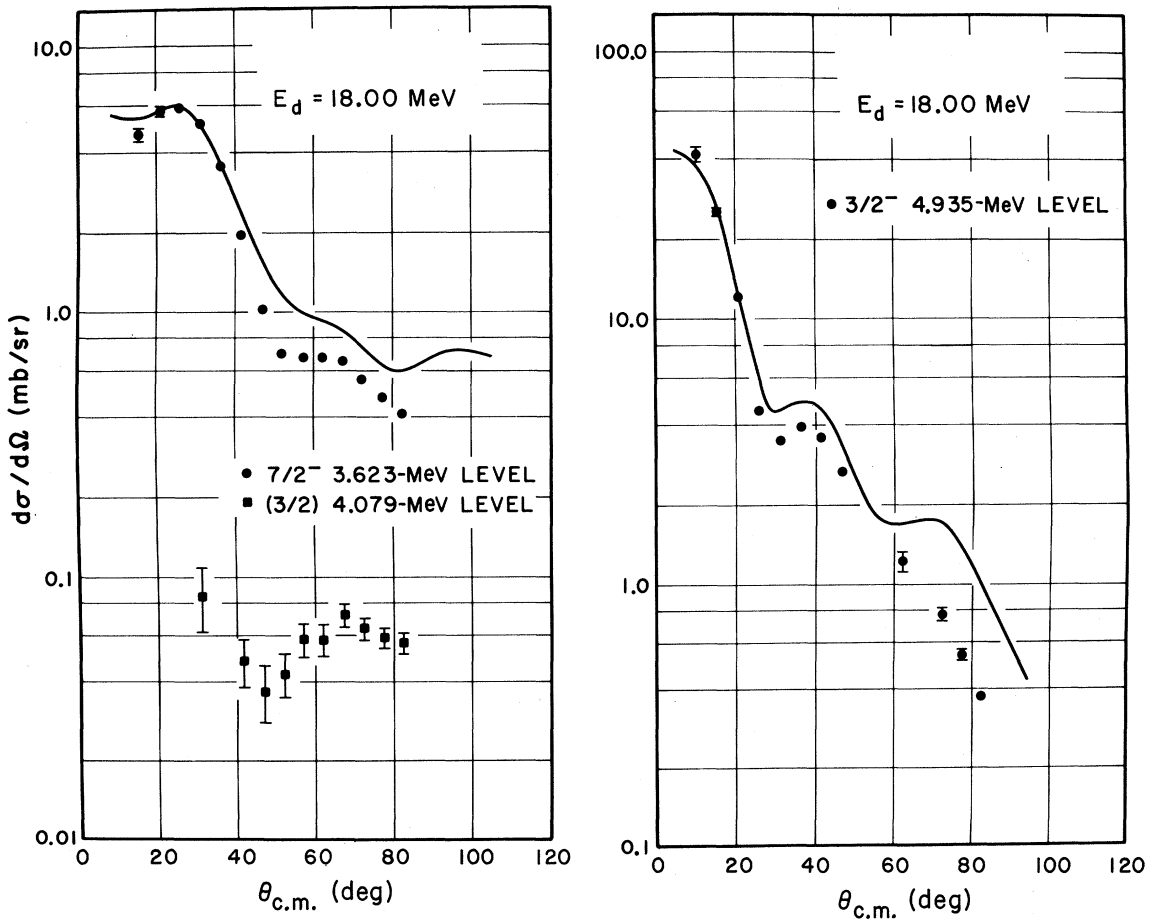

FIG. 3. ^{28}Si$(d,p)^{29}$Si angular distributions for the $\frac{7}{2}^-$ 3.623-, the $(\frac{3}{2})$ 4.079-, and the $\frac{3}{2}^-$ 4.935-MeV levels. The solid curves represent an $l=3$, $1f_{7/2}$ DWBA fit for the (d,p) transition to the 3.623-MeV level and an $l_n=1$, $2p_{3/2}$ DWBA fit in the case of the 4.935-MeV state.

(Fig. 5) were normalized by a common factor to give approximately the same spectroscopic factors determined at 18.00 MeV. This factor was then used to normalize the DWBA curves for the transitions to the 5.944-, 6.195-, and 6.382-MeV levels. The spectroscopic factors obtained by this procedure are presented in Table III. These spectroscopic factors agree reasonably well with those obtained by Betigeri *et al.*[7] at $E_d = 15.00$ MeV, except for the $l=2$ (d, p) transition to the 5.944-MeV $(\frac{3}{2}^+, \frac{5}{2}^+)$ level, where the present experiment's $(2J+1)S$ value of 0.22 is much smaller than the $(2J+1)S$ value of 0.57 obtained in the $E_d = 15.00$ MeV experiment.[7]

D. Reaction $^{32}S(d, p)^{33}S$ at 18.00 MeV

Figure 6 presents the experimental proton spectrum obtained in the reaction $^{32}S(d, p)^{33}S$ at $E_d = 18.00$ MeV and a lab angle of 25°. Proton groups were observed corresponding to the formation of levels in ^{33}S up to an excitation energy of approximately 7.75 MeV. The $^{32}S(d, p)$ angular distributions resulting from the analysis of these data are presented in Figs. 7–11, while the spectroscopic factors are listed in Table IV. The (d, p) angular distributions for ^{33}S levels with excitation energies less than 5 MeV were analyzed out to about 90°, while the angular distributions for most levels above 5 MeV were analyzed only out to 40°. In the following discussion of these data we will emphasize the new and distinctive results of the present experiment.

Figure 7 presents the (d, p) angular distributions associated with the formation of three known $\frac{3}{2}^+$ or $\frac{5}{2}^+$ levels in ^{33}S. The transitions to the $\frac{3}{2}^+$ ground state and $\frac{3}{2}^+$ 2.313-MeV level show definite $l=2$ stripping patterns, well fitted by DWBA curves, while the transition to the $\frac{5}{2}^+$ 1.968-MeV level shows no evidence for a forward-angle stripping pattern. With regard to the relative forward-an-

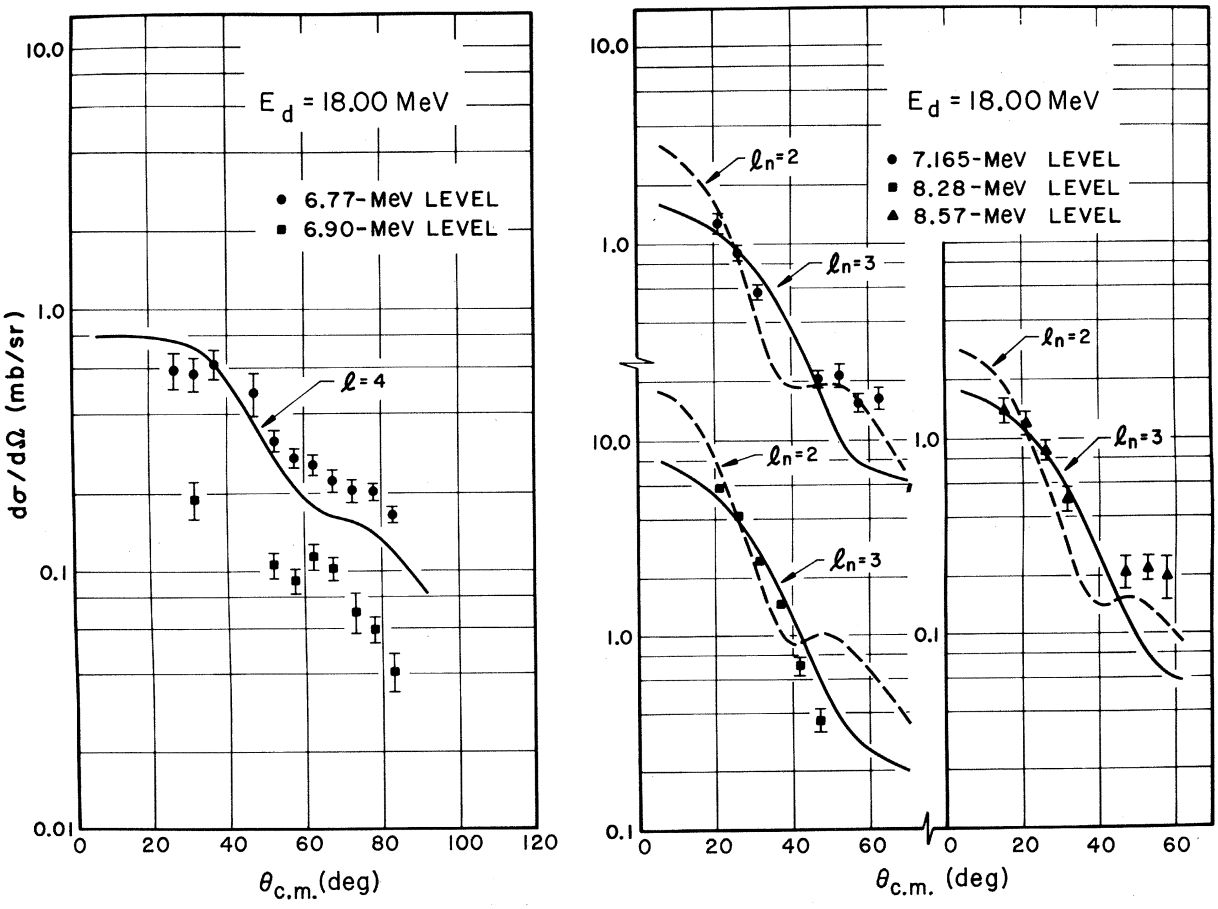

FIG. 4. $^{28}Si(d,p)^{29}Si$ angular distributions for the 6.77-, 6.90-, 7.165-, 8.28-, and 8.57-MeV levels. The solid curve represents an $l=4$, $1g_{9/2}$ DWBA fit for the (d,p) transition to the 6.77-MeV level. In the latter three cases, the solid and dashed curves represent respective $l=3$ and $l=2$ DWBA fits. The 8.57-MeV state is unbound for neutron emission by about 90 keV; the DWBA curves for the transition to this level represent (d,p) transitions to a just bound level in ^{29}Si.

TABLE II. Spectroscopic factors for the reaction $^{28}Si(d,p)^{29}Si$ at $E_d = 18.00$ MeV.

E_x [a] (MeV)	J^π	l	$(2J+1)S$	S
0	$\frac{1}{2}^+$	0	1.05	0.53
1.273	$\frac{3}{2}^+$	2	2.95	0.74
2.032	$\frac{5}{2}^+$	2	0.73	0.12
2.427	$\frac{3}{2}^+$	n.s. [b]	<0.05	<0.012
3.069	$\frac{5}{2}^+$	2	0.35	0.06
3.623	$\frac{7}{2}^-$	3	3.00	0.38
4.935	$\frac{3}{2}^-$	1	2.25	0.56
6.77 ± 0.02	$(\frac{9}{2}^+)$	(4)	0.60	0.06
7.165 ± 0.02	$(\frac{3}{2}^+)$	(2)	(0.32) [c]	(0.08) [c]
	$(\frac{5}{2}^-)$	(3)	(0.40) [d]	(0.07) [d]
8.28 ± 0.02	$(\frac{3}{2}^+)$	(2)	(1.40) [c]	(0.35) [c]
	$(\frac{5}{2}^-)$	(3)	(1.33) [d]	(0.22) [d]
8.57 ± 0.02	$(\frac{3}{2}^+)$	(2)	(0.20) [c]	(0.05) [c]
	$(\frac{5}{2}^-)$	(3)	(0.28) [d]	(0.05) [d]

[a] All excitation energies without error bars are taken from Ref. 5 and are accurate to better than ±4 keV. The excitation energies with error bars were determined in the present work.

[b] Nonstripping.

[c] If the spin of this level is $\frac{5}{2}^+$ rather than $\frac{3}{2}^+$, multiply $(2J+1)S$ by 0.75 and multiply S by 0.50.

[d] If the spin of this level is $\frac{7}{2}^-$ rather than $\frac{5}{2}^-$, multiply $(2J+1)S$ by 0.70 and multiply S by 0.50.

TABLE III. Spectroscopic factors for the reaction $^{28}Si(d,p)^{29}Si$ at $E_d = 21.00$ MeV.

E_x [a] (MeV)	J^π	l	$(2J+1)S$ [b]	S	$S(E_d = 18.00$ MeV)
3.623	$\frac{7}{2}^-$	3	3.25	0.41	0.38
4.935	$\frac{3}{2}^-$	1	2.20	0.55	0.56
5.944	$(\frac{3}{2}^+)$	2	(0.22)	(0.055)	
	$(\frac{5}{2}^+)$		(0.165)	(0.028)	
6.195	$(\frac{5}{2}^-)$	3	(1.75)	(0.29)	
	$(\frac{7}{2}^-)$		(1.20)	(0.15)	
6.382	$\frac{1}{2}^-$	1	1.05	0.53	

[a] All excitation energies are taken from Ref. 5 and are accurate to better than ±4 keV.

[b] As is discussed in the text, the spectroscopic factors at $E_d = 21.00$ MeV were obtained by a normalization procedure which used the strong (d,p) transitions to the $\frac{7}{2}^-$ 3.623-MeV and $\frac{3}{2}^-$ 4.935-MeV levels in ^{29}Si as calibrations. In this normalization procedure the (d,p) transition to the $\frac{3}{2}^-$ 4.935-MeV level was given more weight, since the DWBA fit for this transition was better than that for the $\frac{7}{2}^-$ 3.623-MeV (d,p) transition.

TABLE IV. Spectroscopic factors for the reaction $^{32}S(d,p)^{33}S$ at $E_d = 18.00$ MeV.

E_x [a] (MeV)	J^π	l	$(2J+1)S$	S
0	$\frac{3}{2}^+$	2	3.70	0.93
0.842	$\frac{1}{2}^+$	0	0.63	0.32
1.968	$\frac{5}{2}^+$	n.s.	<0.011	<0.002
2.313	$\frac{3}{2}^+$	2	0.265	0.066
2.869 [b]	$(\frac{3}{2}^+)$	2	(0.40)	(0.10)
	$(\frac{5}{2}^+)$		(0.30)	(0.05)
2.937	$\frac{7}{2}^-$	3	4.50	0.57
3.221	$\frac{3}{2}^-$	1	1.90	0.48
4.213	$\frac{3}{2}^-$	1	0.30	0.075
4.920 [c]	$\frac{1}{2}^-$ [d]	1	0.088	0.044
4.941 [c]	$(\frac{5}{2}^-)$	3	(0.42)	(0.07)
	$(\frac{7}{2}^-)$		(0.29)	(0.036)
5.715	$\frac{1}{2}^-$	1	1.06	0.53
5.894	$\frac{3}{2}^-$	1	0.44	0.11
6.428	$(\frac{1}{2}^-)$	1	(0.35)	(0.18)
	$(\frac{3}{2}^-)$		(0.32)	(0.08)
6.692 ± 0.009	$(\frac{5}{2}^-)$	3	(1.05) [e]	(0.18) [e]
7.193	$\frac{3}{2}^-$	1	0.184	0.046
7.44 group	$(\frac{1}{2}^-)$	1	(0.53)	(0.26)
	$(\frac{3}{2}^-)$		(0.48)	(0.12)
7.61 ± 0.02	$(\frac{5}{2}^-)$	3	(0.32) [e]	(0.053) [e]

[a] All excitation energies without error bars are taken from Ref. 5 and are accurate to better than ±6 keV. The excitation energies with error bars were determined in the present work.

[b] The spectroscopic factor for this level is based on forward-angle data between 10 and 17° where the 2.869-MeV level could be resolved from the more strongly excited 2.937-MeV level.

[c] The 4.920-4.941-MeV doublet (Ref. 19) was not resolved in our data. However, the summed experimental (d,p) angular distribution between 10 and 40° was separated into distinct $l=1$ and $l=3$ components (see text).

[d] Reference 18.

[e] If the spin of this level is $\frac{7}{2}^-$ rather than $\frac{5}{2}^-$, multiply $(2J+1)S$ by 0.70 and multiply S by 0.50.

TABLE V. Spectroscopic factors for the reaction $^{34}S(d,p)^{35}S$ at $E_d = 18.00$ MeV.

E_x [a] (MeV)	J^π	l	$(2J+1)S$	S
0	$\frac{3}{2}^+$	2	1.85	0.46
1.992 ± 6	$\frac{7}{2}^-$	3	5.05	0.63
2.348 ± 2	$\frac{3}{2}^-$	1	2.00	0.50

[a] Reference 5.

gle excitation of these three levels, it is quite interesting to compare the present 18.00-MeV (d, p) experiment with a previous (d, p) experiment at a lower incident deuteron energy. At 20° and 18.00 MeV (Fig. 6) the $\frac{3}{2}^+$ ground state, $\frac{3}{2}^+$ 2.313-MeV level, and $\frac{5}{2}^+$ 1.968-MeV level are excited in the proportions 100:11:0.4. A previous 9-MeV $^{32}S(d, p)$ experiment[17] found that these three levels were excited in the proportions 100:20:5 at the maximum of the $l=2$ stripping pattern (~28°). In the 9-MeV (d, p) experiment the $\frac{3}{2}^+$ ground state and $\frac{3}{2}^+$ 2.313-MeV level showed $l=2$ stripping patterns, while the cross section to the $\frac{5}{2}^+$ 1.968-MeV level was constant to within a factor of 2 between 15 and 150°. The very weak excitation of the 1.968-MeV level in the present 18.00-MeV (d, p) data places a quite small upper limit on the stripping strength to this level.

The summed (d, p) angular distribution to the $(\frac{3}{2}^+, \frac{5}{2}^+)$ 2.869-MeV, $\frac{7}{2}^-$ 2.937-MeV, and 2.970-MeV triplet of levels (Fig. 8) is dominated by the strong $l=3$ transition to the $\frac{7}{2}^-$ 2.937-MeV level. However, the yield to the $(\frac{3}{2}^+, \frac{5}{2}^+)$ 2.869-MeV level could be resolved at the very forward angles (10, 14, and 17°); these three data points give a fairly accurate measurement of the $l=2$ strength to the 2.869-MeV level. The 3.832-MeV level is excited quite weakly by the (d, p) reaction at 18.00 MeV. From 25 to 40° it is excited with $\sim\frac{1}{100}$ the strength of the (d, p) transition to the $\frac{7}{2}^-$ 2.937-MeV level. This is in contrast to lower energy $^{32}S(d, p)$ work,[5] where the 3.832-MeV level is excited with $\sim\frac{1}{10}$ the

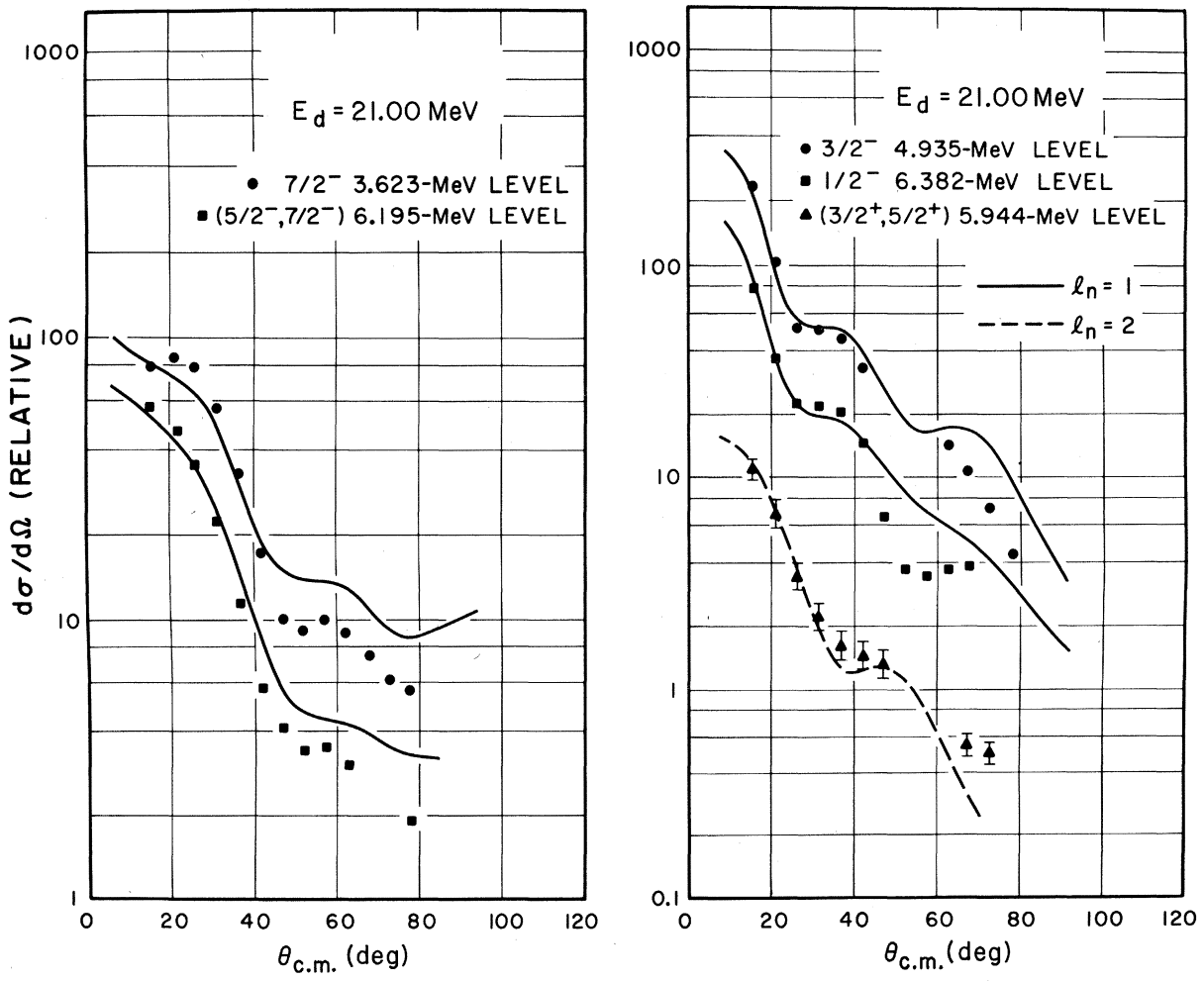

FIG. 5. $^{28}Si(d,p)^{29}Si$ angular distributions for the $\frac{7}{2}^-$ 3.623-, the $(\frac{5}{2}^-, \frac{7}{2}^-)$ 6.195-, the $\frac{3}{2}^-$ 4.935-, the $\frac{1}{2}^-$ 6.382-, and the $(\frac{3}{2}^+, \frac{5}{2}^+)$ 5.944-MeV levels at $E_d=21.00$ MeV. The solid curves represent $l=3$, $1f_{7/2}$ and $1f_{5/2}$ DWBA fits for the (d,p) transitions to the 3.623- and 6.195-MeV levels, respectively, and $l=1$, $2p_{3/2}$ and $2p_{1/2}$ DWBA fits in the respective 4.935- and 6.382-MeV cases. The dashed curves represents an $l=2$, $1d_{3/2}$ DWBA fit for the (d,p) transition to the 5.944-MeV level.

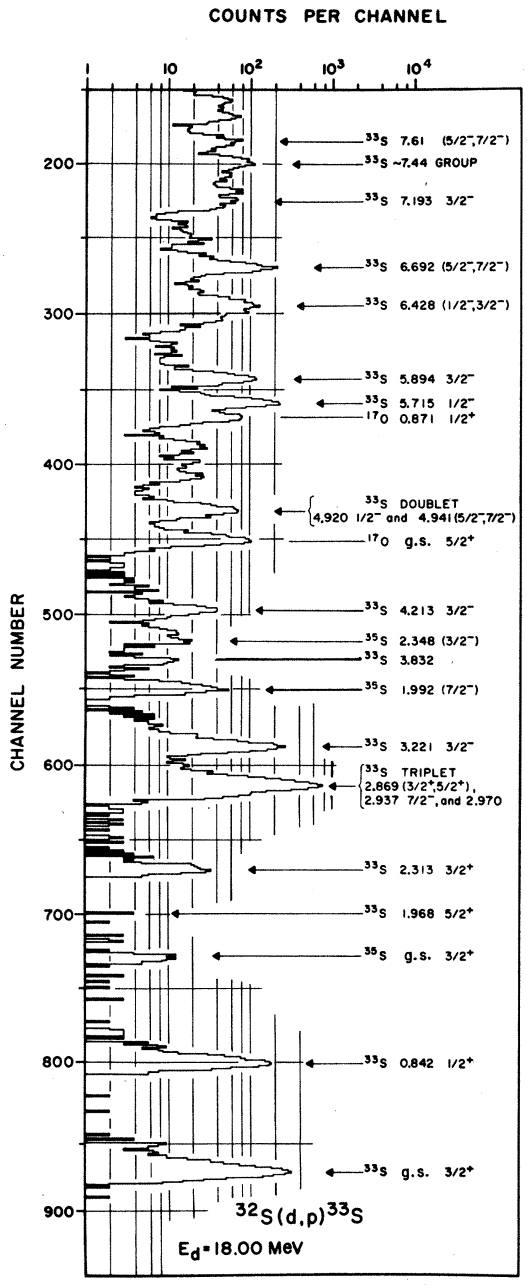

FIG. 6. Experimental proton spectrum at $\theta_{lab} = 25°$ from the bombardment of 18.00-MeV deuterons on a natural sulfur target (^{32}S 95.06%, ^{33}S 0.75%, ^{34}S 4.18%, and ^{36}S 0.014%). Most of the experimentally observed (d,p) transitions correspond to the reaction ^{32}S$(d,p)^{33}$S (Q_m = +6.417 MeV), although a few transitions correspond to the reaction ^{34}S$(d,p)^{35}$S (Q_m = +4.761 MeV) and also the reaction ^{16}O$(d,p)^{17}$O from a small oxygen contamination in the H_2S gas target.

strength of the 2.937-MeV level.

^{33}S levels have been reported at excitation energies of 4.920 and 4.941 MeV,[5] and the spin of the 4.920-MeV level is known to be $\frac{1}{2}^-$.[18] Recent high-resolution $S(d, p)$ work at $E_d = 6.0$ MeV has resolved these two levels; and the angular distribution to the 4.941-MeV level is consistent with an $l = 3$ assignment.[19] In our data the angular distribution for the proton group corresponding to an excitation energy of 4.92 MeV in ^{33}S (Fig. 9) is definitely not a pure $l = 1$ transition. The $l = 1$ (d, p) angular distributions to known $\frac{1}{2}^-$ and $\frac{3}{2}^-$ lev-

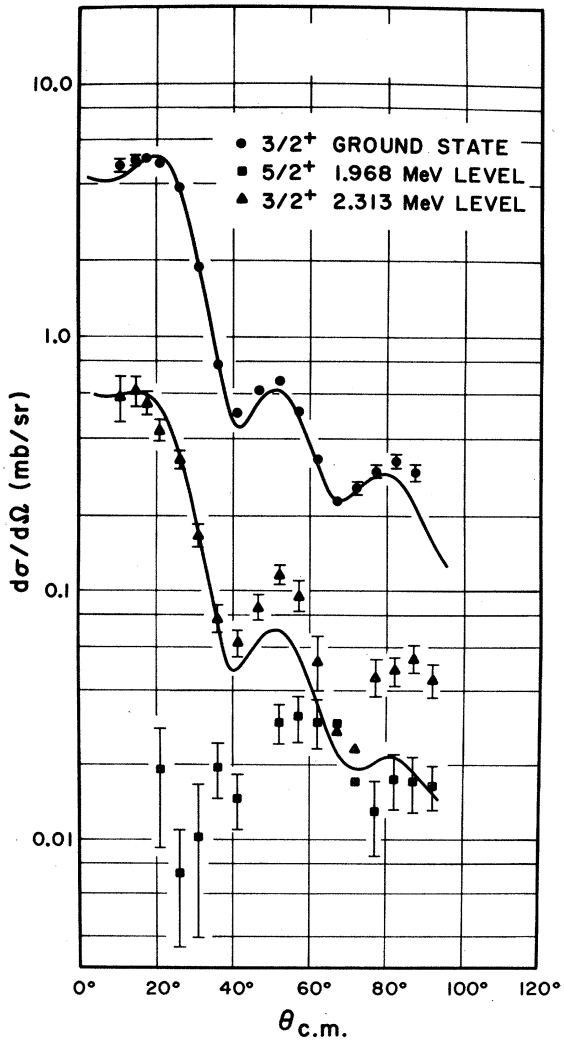

FIG. 7. ^{32}S$(d,p)^{33}$S angular distributions for the $\frac{3}{2}^+$ ground state, the $\frac{5}{2}^+$ 1.968-MeV level, and the $\frac{3}{2}^+$ 2.313-MeV level. The solid curves represent $l = 2$, 1d DWBA fits for the (d,p) transitions to the $\frac{3}{2}^+$ ground state and the $\frac{3}{2}^+$ 2.313-MeV level. The (d,p) transition to the $\frac{5}{2}^+$ 1.968-MeV level shows no evidence for a forward-angle stripping pattern.

TABLE VI. Spectroscopic factors for the reaction $^{36}Ar(d,p)^{37}Ar$.

	Present work $E_d = 18.00$ MeV				Sen, Hollas, and Riley (Ref. 23) $E_d = 9.162$ MeV				Rosner and Schneid (Ref. 8) $E_d = 15.0$ MeV			
E_x [a] (MeV)	l	J^π	$(2J+1)S$	S	E_x [b] (MeV)	l	J^π	S	E_x	l	J^π	S
0	2	$\frac{3}{2}^+$	2.06	0.52	0	2	$\frac{3}{2}^+$	0.49	0	2	$\frac{3}{2}^+$	0.43
1.409	0	$\frac{1}{2}^+$	0.19	0.10	1.402	0	$\frac{1}{2}^+$	0.22	1.40	0	$\frac{1}{2}^+$	0.14
1.611	3	$\frac{7}{2}^-$	6.19	0.77	1.606	3	$\frac{7}{2}^-$	0.51	1.60	3	$\frac{7}{2}^-$	0.82
2.491	1	$\frac{3}{2}^-$	1.67	0.42	2.481	1	$\frac{3}{2}^-$	0.35	2.50	1	$\frac{3}{2}^-$	0.45
2.796	2	$\frac{5}{2}^+$	0.23	0.040	2.788	2	$\frac{5}{2}^+$	0.06				
3.516	1	$\frac{3}{2}^-$	1.31	0.33	3.511	1	$\frac{3}{2}^-$	0.23	3.55	1	$\frac{3}{2}^-$	0.36
					3.595	1	$\frac{3}{2}^-$	0.01				
					4.391	3	$\frac{7}{2}^-$	0.03				
4.466	1	$\frac{1}{2}^-$	0.29	0.14	4.441	1	$\frac{1}{2}^-$	0.14	4.46	1	$\frac{1}{2}^-$	0.16
4.657	(3)	$(\frac{5}{2}^-)$	(0.096)	(0.016) [c]	4.623	1	$\frac{3}{2}^-$	0.02				
4.764	(3)	$(\frac{5}{2}^-)$	(0.072)	(0.012) [c]	4.735	1	$\frac{3}{2}^-$	0.02				
5.110	1	$\frac{1}{2}^-$	1.03	0.51	5.082	1	$\frac{1}{2}^-$	0.49	5.18	1	$\frac{1}{2}^-$	0.59
5.241	(3)	$(\frac{5}{2}^-)$	(0.180)	(0.030) [c]	5.209	1	$\frac{3}{2}^-$	0.02				
5.376	1	$\frac{1}{2}^-$	0.15	0.075	5.339	1	$(\frac{1}{2}^-)$	0.08				
		$\frac{3}{2}^-$	0.15	0.038								
5.439 5.467	(3)	$(\frac{5}{2}^-)$	(0.180)	(0.030) [c]	5.429	1	$(\frac{1}{2}^-)$	0.03				
					5.598	1	$\frac{1}{2}^-$	0.02				
					5.961	1	$(\frac{3}{2}^-)$	0.01				
6.164	1	$\frac{1}{2}^-$	0.058	0.029	6.135	1	$(\frac{1}{2}^-)$	0.05				
		$\frac{3}{2}^-$	0.055	0.014	6.204	1	$\frac{1}{2}^-$	0.05				
6.314	3	$\frac{5}{2}^-$	0.67	0.11	6.289	3	$\frac{7}{2}^-$	0.11				
		$\frac{7}{2}^-$	0.44	0.055								
6.452 6.472	3	$\frac{5}{2}^-$	0.36	0.060	In the experiment of Ref. 23 this region was masked by the elastic deuteron group.							
		$\frac{7}{2}^-$	0.25	0.031								
6.588 6.604	3	$\frac{5}{2}^-$	1.06	0.18								
		$\frac{7}{2}^-$	0.70	0.088								
6.952	1	$\frac{1}{2}^-$	0.13	0.065								
		$\frac{3}{2}^-$	0.13	0.033								
7.162	3	$\frac{5}{2}^-$	0.21	0.035	7.131	1	$\frac{1}{2}^-$	0.05				
		$\frac{7}{2}^-$	0.14	0.018								
7.255 7.263 7.286	3	$\frac{5}{2}^-$	1.03	0.17	7.246	1	$\frac{1}{2}^-$	0.05				
		$\frac{7}{2}^-$	0.70	0.088								

TABLE VI *(Continued)*

Present work $E_d = 18.00$ MeV					Sen, Hollas, and Riley (Ref. 23) $E_d = 9.162$ MeV				Rosner and Schneid (Ref. 8) $E_d = 15.0$ MeV			
E_x [a] (MeV)	l	J^π	$(2J+1)S$	S	E_x [b] (MeV)	l	J^π	S	E_x	l	J^π	S
7.612	1	$\frac{1}{2}^-$	0.19	0.095	7.571	1	$\frac{1}{2}^-$	0.08				
		$\frac{3}{2}^-$	0.19	0.050								
7.906	1	$\frac{1}{2}^-$	0.39	0.20	7.895 [d]	1	$\frac{1}{2}^-$	0.07				
		$\frac{3}{2}^-$	0.39	0.10								

[a] For $E_x \leq 3.516$ MeV, the experimental levels were correlated with the excitation energies of Ref. 20, which have uncertainties of ±2 keV. For $E_x > 3.516$ MeV, the experimental levels were correlated with the excitation energies of Ref. 21, which have uncertainties of ±10 keV.

[b] The excitation energies have an error of ±20 keV.

[c] If the spin is $\frac{7}{2}^-$, $S(\frac{7}{2}^-) = 0.5S(\frac{5}{2}^-)$.

[d] Reference 23 also presents data for five $l_n = 1(d, p)$ transitions with excitation energies between 8.0 and 9.1 MeV.

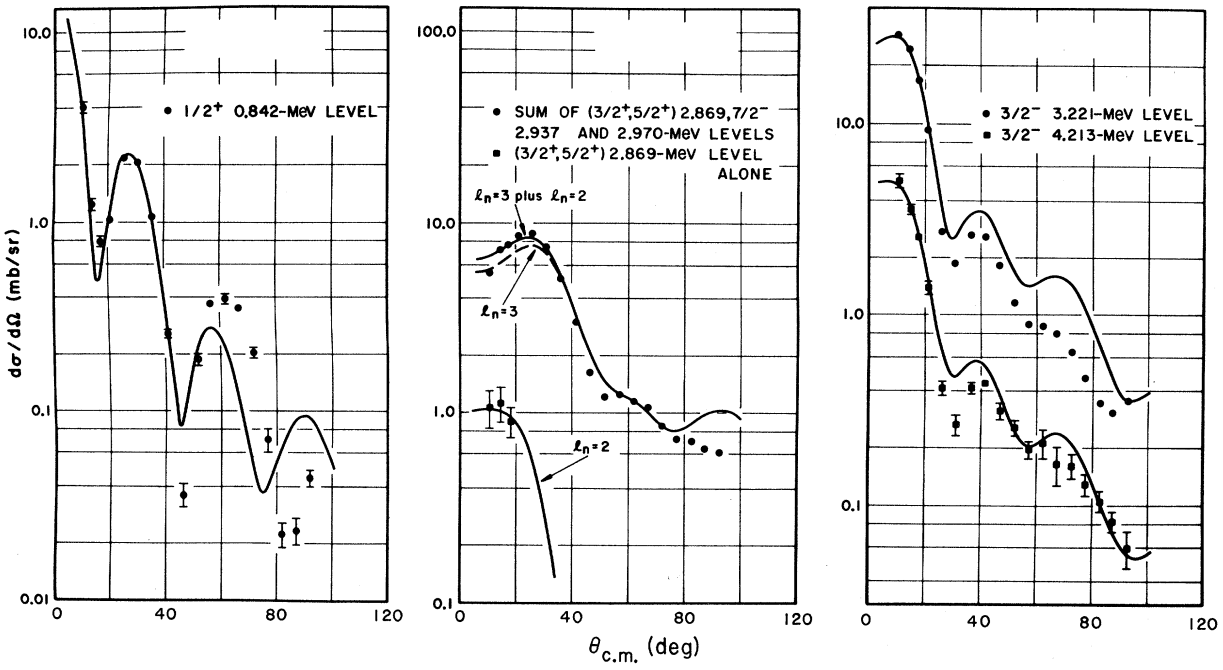

FIG. 8. $^{32}S(d,p)^{33}S$ angular distributions for the $\frac{1}{2}^+$ 0.842-MeV level, the $(\frac{3}{2}^+, \frac{5}{2}^+)$ 2.869-MeV, $\frac{7}{2}^-$ 2.937-MeV, 2.970-MeV composite of levels, the $\frac{3}{2}^-$ 3.221-MeV level, and the $\frac{3}{2}^-$ 4.213-MeV level. The solid curve represents an $l = 0$, $2s_{1/2}$ DWBA fit for the (d,p) transition to the 0.842-MeV level. In the case of the three level composite, at three forward angles the contribution to the 2.869-MeV level could be resolved and these three points are also displayed. The $l = 2$ spectroscopic strength to the 2.869-MeV level is determined by an $l = 2$, $1d$ DWBA curve fitted to these three forward-angle points. The summed angular distribution is fitted with an $l = 3$, $1f_{7/2}$ DWBA curve (dotted line) and a solid curve which represents the sum of this $l = 3$ curve and the $l = 2$ curve indicated by the forward-angle cross section to the 2.869-MeV level. Any contribution from the (d,p) transition to the 2.970-MeV level is neglected in this analysis. For the 3.221- and 4.213-MeV cases, the solid curves represent $l = 1$, $2p_{3/2}$ DWBA fits.

els with excitation energies less than and greater than 4.92 MeV (see Figs. 8 and 10) fall off much more rapidly between 15 and 30° than the (d, p) angular distribution presented in Fig. 9. However, between 10 and 40° this angular distribution can be fitted quite nicely by the sum of $l=1$ and $l=3$ DWBA curves. Therefore we have assumed that the proton group presented in Fig. 9 corresponds to two (d, p) transitions: an $l=1$ transition to the $\frac{1}{2}^-$ 4.920-MeV level in ^{33}S, and an $l=3$ transition to the 4.941-MeV level in ^{33}S.

Five (d, p) angular distributions (Fig. 10) to ^{33}S levels with excitation energies between 5.5 and 7.5 MeV are well fitted by $l=1$ DWBA curves. $l=1$ (d, p) transitions have been previously reported to the 5.715- and 5.894-MeV levels of ^{33}S[5]; the $l=1$ (d, p) transitions to the 6.428-, 7.193-, and 7.44-MeV levels are new findings of the present experiment. In the ^{33}S excitation energy region between 6.0- and 8.0-MeV ^{32}S thermal-neutron-capture experiments[5] have identified four levels in ^{33}S at 6.428, 6.890, 7.193, and 7.421 MeV; and one would expect that the spins of these levels would be $\frac{1}{2}^-$ or $\frac{3}{2}^-$, since the $\frac{1}{2}^+$ thermal-neutron

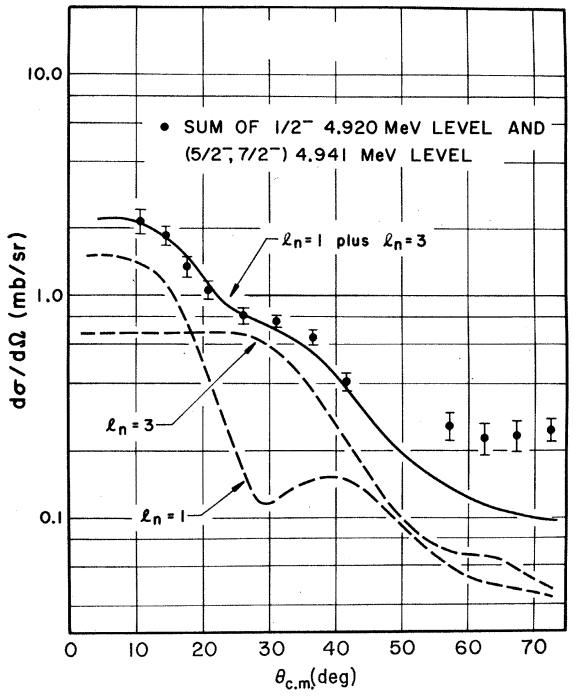

FIG. 9. ^{32}S$(d,p)^{33}$S angular distribution for a proton group corresponding to an excitation energy of 4.92 MeV in ^{33}S. This transition is well fitted by a curve (solid) which represents the sum of $l=1$, $2p$ and $l=3$, $1f$ DWBA curves (dashed). As is discussed in the text, this angular distribution most probably represents the sum of an $l=1$ (d,p) transition to the $\frac{1}{2}^-$ 4.920 level and an $l=3$ (d,p) transition to the $(\frac{5}{2}^-, \frac{7}{2}^-)$ 4.941 level.

plus ^{32}S system would preferentially excite $\frac{1}{2}^-$ or $\frac{3}{2}^-$ levels in ^{33}S by $E1$ γ transitions. γ-γ angular-correlation experiments have established spin assignments of $\frac{3}{2}$ and $(\frac{1}{2}, \frac{3}{2})$ for the 7.193- and 7.421-MeV levels, respectively.[5] We can match three of these four levels with reasonably strong $l=1$ (d, p) transitions (Fig. 10). The exception is the 6.890-MeV level reported in the thermal-neutron-capture experiments. In the present 18-MeV (d, p) data this level is excited with less than ~0.25 the strength of the 7.193-MeV level (Fig. 10). In the analysis of the (d, p) angular distribution to the 6.428-MeV level there is some error involved in separating this level from another level at ~6.34 MeV. The level at ~6.34 MeV is excited with some strength at angles greater than 20° (see Fig. 6). However, for angles less than 20° only the 6.428-MeV level is strongly excited; and its angular distribution (Fig. 10) is consistent with a pure $l=1$ (d, p) transition. The proton group whose mean energy corresponds to an excitation energy of 7.44 ± 0.02 MeV does not correspond to a single level in ^{33}S, since its width exceeds the experimental resolution. However, the (d, p) angular distribution for this group is consistent with a pure $l=1$ transition (see Fig. 10). To a good degree of certainty, this group would include the 7.421-MeV level seen in thermal-neutron-capture experiments.

A ^{33}S level at 6.692 ± 0.009 MeV is excited quite strongly in the (d, p) reaction and its angular dis-

TABLE VII. Comparison of the experimental summed spectroscopic strengths, $\sum (2J+1)S$, for $2s$-$1d$, $1f$, and $2p$ transfer in the ^{28}Si, ^{32}S, and ^{36}Ar(d, p) reactions and the simple-shell-model prediction.

Target	$\sum(2J+1)S$	Simple-shell-model prediction
^{28}Si		
$2s$-$1d$ transitions	5.3 [a]	6.0
$1f$ transitions	6.2 [b]	14.0
$2p$ transitions	3.3	6.0
^{32}S		
$2s$-$1d$ transitions	5.0	4.0
$1f$ transitions	6.0 [b]	14.0
$2p$ transitions	4.8	6.0
^{36}Ar		
$2s$-$1d$ transitions	2.3	2.0
$1f$ transitions	9.4 [b]	14.0
$2p$ transitions	5.2	6.0

[a] This number includes only ^{29}Si levels with $E_x < 6.0$ MeV. There is possible $l_n=2$ strength to levels in ^{29}Si with excitation energies between 7 and 9 MeV. (See Table II and the discussion in Sec. IV B.)

[b] For levels where the spin was unknown (either $\frac{5}{2}^-$ or $\frac{7}{2}^-$), an average value of $(2J+1)S$ for the $l_n=3$ transition was used in forming the sum.

tribution is well fitted by an $l=3$ DWBA curve (Fig. 11). Also, the (d, p) angular distribution to a level at 7.61 ± 0.02 MeV is consistent with an $l=3$ stripping assignment (Fig. 11). The experimental widths of the proton groups to these two levels are consistent with these groups representing single states in ^{33}S. In comparison with the $l=3$ DWBA curve, an $l=2$ DWBA curve gives a decidedly inferior fit for the (d, p) transitions to the 6.692- and 7.61-MeV levels (see Fig. 11). As was discussed in Sec. IV A, the present (d, p) experiment is more sensitive to $l=1$ than $l=3$ spectroscopic strength so that it is very probable that the present analysis has missed some moderately strong $l=3$ (d, p) transitions in the excitation-energy range between 4.0 and 8.0 MeV.

Since the natural sulfur target used in this experiment contained 4.18% ^{34}S, the strong ^{34}S(d, p) transitions to the first three levels of ^{35}S could be analyzed (see Fig. 6). Figure 12 presents the experimental (d, p) angular distributions to the $\frac{3}{2}^+$ ground state, the $\frac{7}{2}^-$ 1.992-MeV level, and the $\frac{3}{2}^-$ 2.348-MeV level of ^{35}S. These transitions are well fitted by $l=2$, $l=3$, and $l=1$ DWBA curves, respectively. The spectroscopic factors obtained from this analysis are presented in Table V.

E. Reaction ^{36}Ar$(d, p)^{37}$Ar at 18.00 MeV

The proton spectrum observed at a lab angle of 25° for the reaction ^{36}Ar$(d, p)^{37}$Ar at $E_d = 18.00$ MeV is shown in Fig. 13. Angular distributions

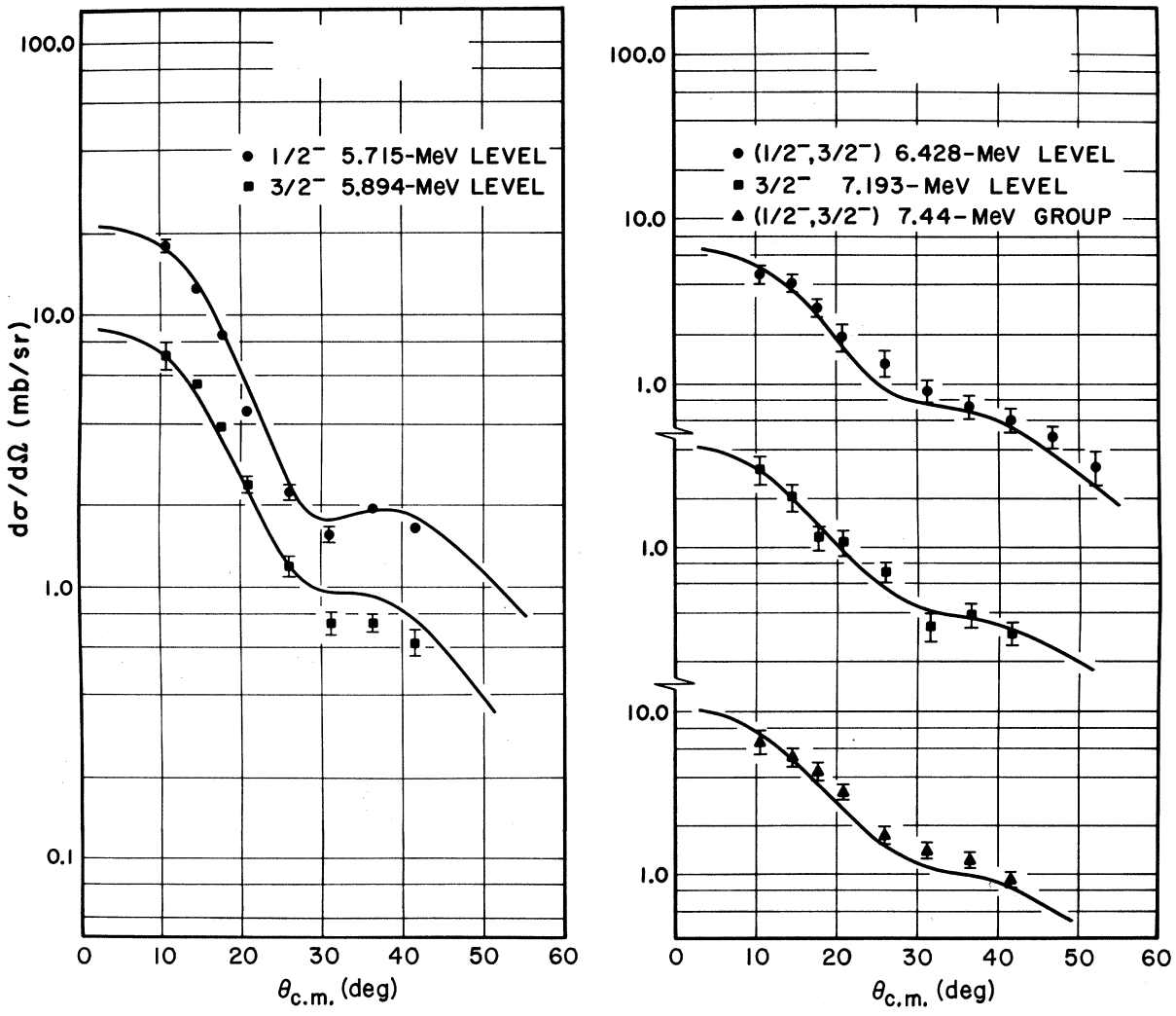

FIG. 10. ^{32}S$(d,p)^{33}$S angular distributions for the $\frac{1}{2}^-$ 5.715-, the $\frac{3}{2}^-$ 5.894-, the $(\frac{1}{2}^-, \frac{3}{2}^-)$ 6.428-, and the $\frac{3}{2}^-$ 7.193-MeV levels and also a multiplet of levels with a mean excitation energy of 7.44 ± 0.02 MeV. The solid curves represent $l=1$, $2p$ DWBA fits for these transitions.

were retrieved from similar spectra that were recorded in the angular range $\theta_{lab} = 10$ to $110°$ for states in ^{37}Ar with $E_x \leq 8.0$ MeV. The excitation energies indicated in Fig. 13 for states with $E_x \leq 3.516$ MeV are those reported by Champlin, Howard, Olness[20] and have uncertainties of ±2 keV; for the higher-lying levels, the values of Holbrow *et al.*[21] are employed (here $\Delta E_x = \pm 10$ keV). The present findings are correlated with these previous ones as indicated in Fig. 13 and Table VI. In those cases where the resolution in the present experiment was unable to distinguish between several possible excitation energies reported in Ref. 21, Table VI lists the experimental (d, p) transition as proceeding to a composite of levels in ^{37}Ar. As is evident in Fig. 13, groups associated with ~1% ^{40}Ar and ^{16}O target impurities are present and correspond to formation of the strongest ^{41}Ar and ^{17}O levels. Upon consideration of the results of ^{40}Ar$(d, p)^{41}$Ar studies carried out at $E_d = 7.5$ [22] and 11.0 MeV,[21] it was concluded that possible contributions to the data other than as indicated in Fig. 13 were negligible. The angular distributions which displayed definitive stripping characteristics are shown in Figs. 14–16 together with the appropriate DWBA fits. The neutron orbital angular momentum transfers and the associated spectroscopic factors are summarized in Table VI, along with the results of two other ^{36}Ar(d, p) experimental studies.[8,23]

Orbital angular momentum transfers and spectroscopic factors have previously been obtained by Rosner and Schneid[8] via a similar experiment carried out at $E_d = 15.0$ MeV for the 0-, 1.409-, 1.611-, 2.491-, 3.516-, 4.466-, and 5.110-MeV ^{37}Ar levels. The present findings concerning these states are in excellent agreement with these previous ones. Sen, Hollas, and Riley (SHR)[23] have recently reported the results of a similar study carried out at $E_d = 9.162$ MeV. As concerns the seven states under discussion, the agreement of spectroscopic factors in some cases is rather poor.

As is illustrated in Fig. 14, the experimental angular distribution corresponding to formation of the 2.796-MeV state is well fitted by an $l_n = 2$ distribution except for the $\theta_{lab} = 10°$ point. Mirror pair identifications[20] strongly suggest that this level possesses $J^\pi = \frac{5}{2}^+$, which is consistent with an $l_n = 2$ transfer. The small spectroscopic factor obtained for this state is in agreement with the findings of SHR.[23] The DWBA fit to the data was not

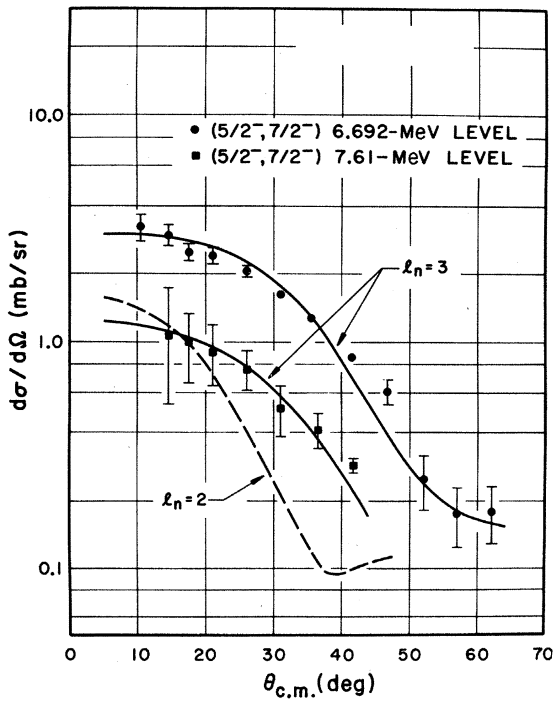

FIG. 11. ^{32}S$(d,p)^{33}$S angular distributions for two levels at 6.692±0.009 and 7.61±0.02 MeV. These (d,p) transitions are well fitted by the solid $l=3$, $1f$ DWBA curves. For the purpose of comparison, a dashed $l=2$, $1d$ DWBA is included.

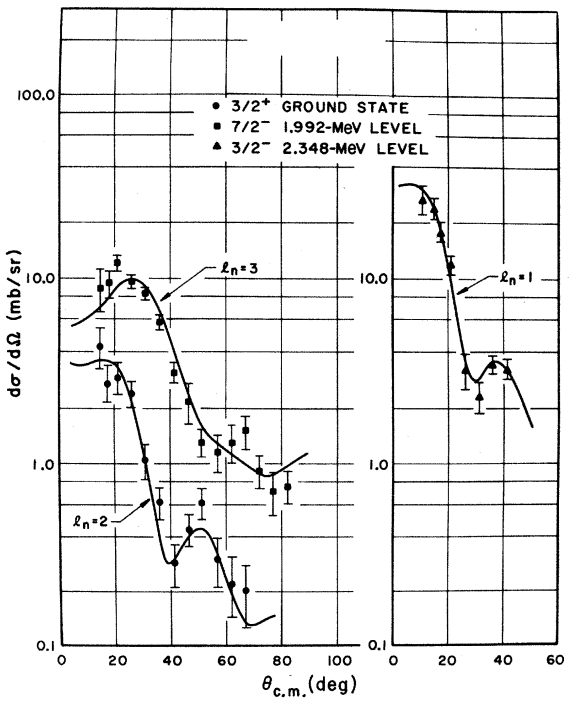

FIG. 12. ^{34}S$(d,p)^{35}$S angular distributions for the first three levels in ^{35}S: the $\frac{3}{2}^+$ ground state, the $\frac{1}{2}^-$ 1.992-MeV level, and the $\frac{3}{2}^-$ 2.348-MeV level. The solid curves represent respective $l=2$, $1d_{3/2}$; $l=3$, $1f_{7/2}$; and $l=1$, $2p_{3/2}$ DWBA fits for these three (d,p) transitions.

improved by assuming the existence of two levels near this excitation energy and admitting an $l_n = 1$ admixture, as was done in the work of Rosner and Schneid.[8]

In addition to the four prominent $l_n = 1$ transfers associated with formation of the $\frac{3}{2}^-$ 2.491-MeV, $\frac{3}{2}^-$ 3.516-MeV, $\frac{1}{2}^-$ 4.466-MeV, and $\frac{1}{2}^-$ 5.110-MeV levels, five weaker $l_n = 1$ transfers were seen in the present study (see Fig. 15). This stripping character for the 5.376-, 6.164-, 7.612-, and 7.906-MeV states is in agreement with the results of SHR.[23] In addition, the present findings indicate $l_n = 1$ transfer in the formation of the 6.952-MeV level. The situation concerning the weaker $l_n = 1$ transfers reported by SHR[23] but not observed in the present work will be discussed at the end of this subsection.

Figure 16 illustrates the evidence for six angular distributions which displayed the signature of $l_n = 3$ transfer. In addition to the $\frac{7}{2}^-$ 1.611-MeV state, the 6.314-MeV level was found to be formed by $l_n = 3$ transfer in both the present work and that of SHR.[23] The present work further indicates such transfer in the formation of the experimentally unresolved 6.452- and 6.472-level composite; the 6.588- and 6.604-level composite; the 7.162-MeV level; and the 7.255-, 7.263-, 7.286-MeV level composite.

Several of the weaker transitions, for which the differential cross sections at the forward maximum were ~0.2 mb/sr, displayed behavior suggestive of $l_n = 3$ transfer. These angular distributions are illustrated in Fig. 17 and correspond to formation of the 4.657-, 4.764-, and 5.241-MeV levels and also the experimentally unresolved 5.439- and 5.467-MeV states. For assumed $1f_{5/2}$ transfers, the spectroscopic factors have values 0.016, 0.012, 0.030, and 0.030 for the respective cases; for assumed $1f_{7/2}$ transfers, these values should be halved. Because of the fact that compound-nuclear and/or second-order direct mechanisms are known to be capable of contributing significantly in such weak transitions, the assignment of l_n values here must be regarded as tentative. This ambiguity is underlined when a comparison is made between the present experiment and the previous experiment of SHR[23] who report weak but definite $l_n = 1$ transfers ($S = 0.02$ to 0.03) for each of these four cases at $E_d = 9.162$ MeV. Also, there is definite disagreement between the present work at $E_d = 18.00$ MeV and the work of SHR[23] concerning the 7.162-MeV level and the 7.255-, 7.263-, and 7.286-MeV composite. In both these cases the present experiment finds $l_n = 3$ transfer while SHR[23] report $l_n = 1$ transfer. Thus, in all, there are six cases of disagreement. This disagreement is both puzzling and disturbing. Although all six transitions are at least an order-of-magnitude weaker than the strongest (d, p) transitions the data of SHR[23] quite unambiguously indicate $l_n = 1$ transfer for these six transitions, while the present experiment quite unambiguously indicates that these transitions are not $l_n = 1$, and are most probably $l_n = 3$. Also, the present experiment places upper limits on possible $l_n = 1$ spectroscopic strength in

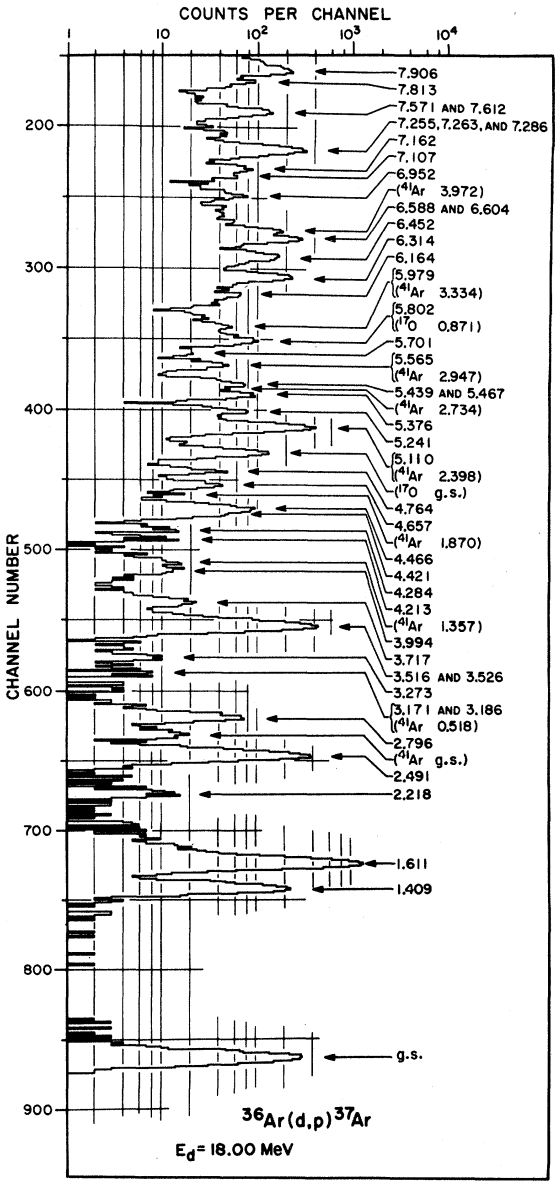

FIG. 13. Experimental proton spectrum at $\theta_{lab} = 25°$ from the bombardment of 18.00-MeV deuterons on an argon gas target (^{36}Ar 98.2%, ^{40}Ar 1.8%). Most of the experimentally observed transitions correspond to the reaction $^{36}\mathrm{Ar}(d,p)^{37}\mathrm{Ar}$ ($Q_m = +6.57$ MeV), although a few transitions correspond to the reaction $^{40}\mathrm{Ar}(d,p)^{41}\mathrm{Ar}$ ($Q_m = +3.87$ MeV) and also the reaction $^{16}\mathrm{O}(d,p)^{17}\mathrm{O}$.

these transitions which are much lower than even the small $l_n = 1$ spectroscopic factors found by SHR.[23] For example, in the present experiment the forward-angle cross sections for the excitation of the 4.657-MeV level indicate $S \leq 0.002$ for possible $l_n = 1$ transfer, while SHR[23] find $S = 0.02$. We made an attempt to explain the cause of these six weak $l_n = 1$ transfers reported in Ref. 23 as an $A \cong 36$ impurity in the gas sample, that is, ^{35}Cl, ^{37}Cl, or ^{38}Ar. The matching of certain strong $l_n = 1$ transitions in the ^{35}Cl, ^{37}Cl, or ^{38}Ar (d, p) reactions[5,24] and some of the six weak $l_n = 1$ (d, p) transitions of Ref. 23 could be accomplished; but no one-to-one correlation could be established. The cause of this discrepancy between the work of Ref. 23 and the present experiment is still an open question.

F. J Dependence

J-dependent effects in the (d, p) angular distributions for $l_n = 2$ $(1d)$ and $l_n = 1$ $(2p)$ transitions have been summarized in two papers by Lee, Schiffer, and co-workers.[17,25] The data on which they based their conclusions were primarily obtained from (d, p) studies with incident deuteron energies between 8 and 13 MeV. In this subsection we would like to compare the effects they observed at these lower energies with our results at 18.00 MeV.

For incident deuteron energies between about 7 and 10 MeV, Lee and Schiffer[25] observed that in the $2s$-$1d$ shell the $l_n = 2$ (d, p) transitions to $J = \frac{3}{2}$ final states exhibited a sharp dropoff from the forward maximum with a minimum at ~55°, while the transitions to $J = \frac{5}{2}$ final states fell off less steeply with no distinct minimum. However, this effect seemed to diminish as the deuteron energy increased.[17,25] Our (d, p) data at 18.00 MeV include six reasonably strong $l_n = 2$ transitions where the spin of the final state is definitely established. These are the transitions to the 1.273-MeV $\frac{3}{2}^+$, 2.032-MeV $\frac{5}{2}^+$, and 3.069-MeV $\frac{5}{2}^+$ levels in ^{29}Si; the $\frac{3}{2}^+$ ground state and 2.313 $\frac{3}{2}^+$ level in ^{33}S; and the $\frac{3}{2}^+$ ground state in ^{37}Ar. The angular distributions for these (d, p) transitions are presented in Figs. 2, 7, and 14. These experimental angular distributions establish a definite forward-angle J dependence for $l_n = 2$ $(1d)$ transitions at 18.00 MeV. The effect is most striking in the angular range from 40 to 60°. The $J = \frac{3}{2}$ transitions have a definite minimum at ≃40° with a secondary maximum at ≃50°. On the other hand the (d, p) angular distributions to $J = \frac{5}{2}$ levels are almost flat between 40 and 58°. Somewhat similar $l = 2$ J dependence has been reported in the Si (d, p) work of Betigeri *et al.* at 15 MeV.[7] This J-dependent effect would indicate that the favored[20] $J^\pi = \frac{5}{2}^+$ assignment for the 2.796-MeV level in ^{37}Ar is correct. [The (d, p) angular distribution to this level is quite flat between 40 and 55° (Fig. 14).]

The $l_n = 1$ $(2p)$ J dependence established by Lee and Schiffer[25] was essentially a backward-angle effect. In target nuclei with $40 < A < 65$ and for deuteron energies between 7 and 12 MeV the $J = \frac{1}{2}$ (d, p) transitions displayed a deep minimum somewhere between 90 and 140° while the $J = \frac{3}{2}$ transitions did not show such an effect. In our 18-MeV experi-

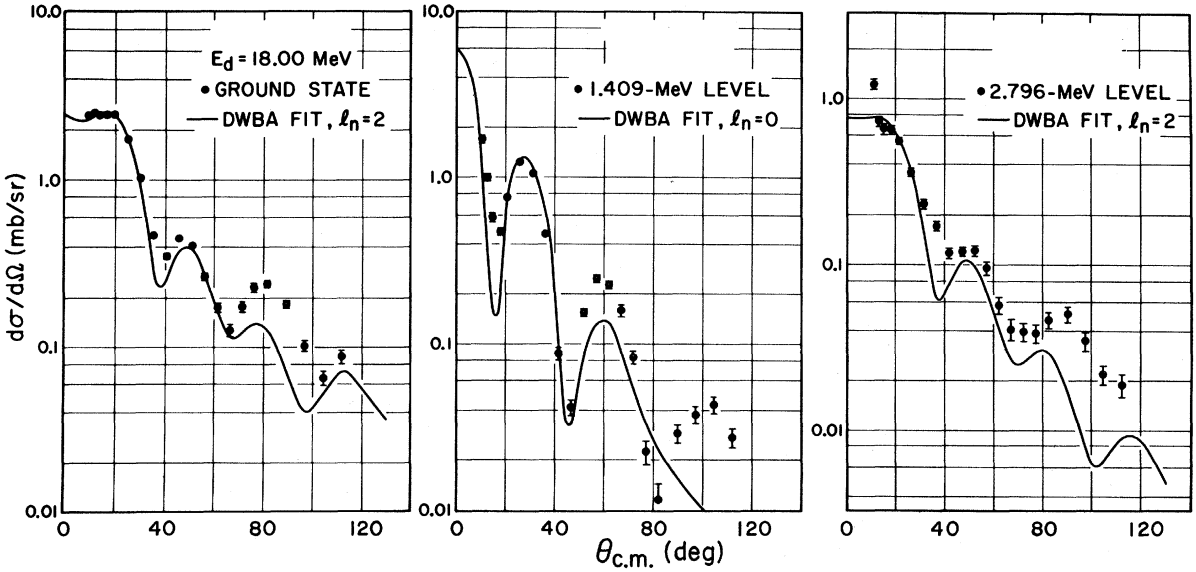

FIG. 14. ^{36}Ar$(d,p)^{37}$Ar angular distributions for the $\frac{3}{2}^+$ ground state, the $\frac{1}{2}^+$ 1.409-MeV level, and the $\frac{5}{2}^+$ 2.796-MeV level. The solid curves represent appropriately labeled DWBA fits for these (d,p) transitions.

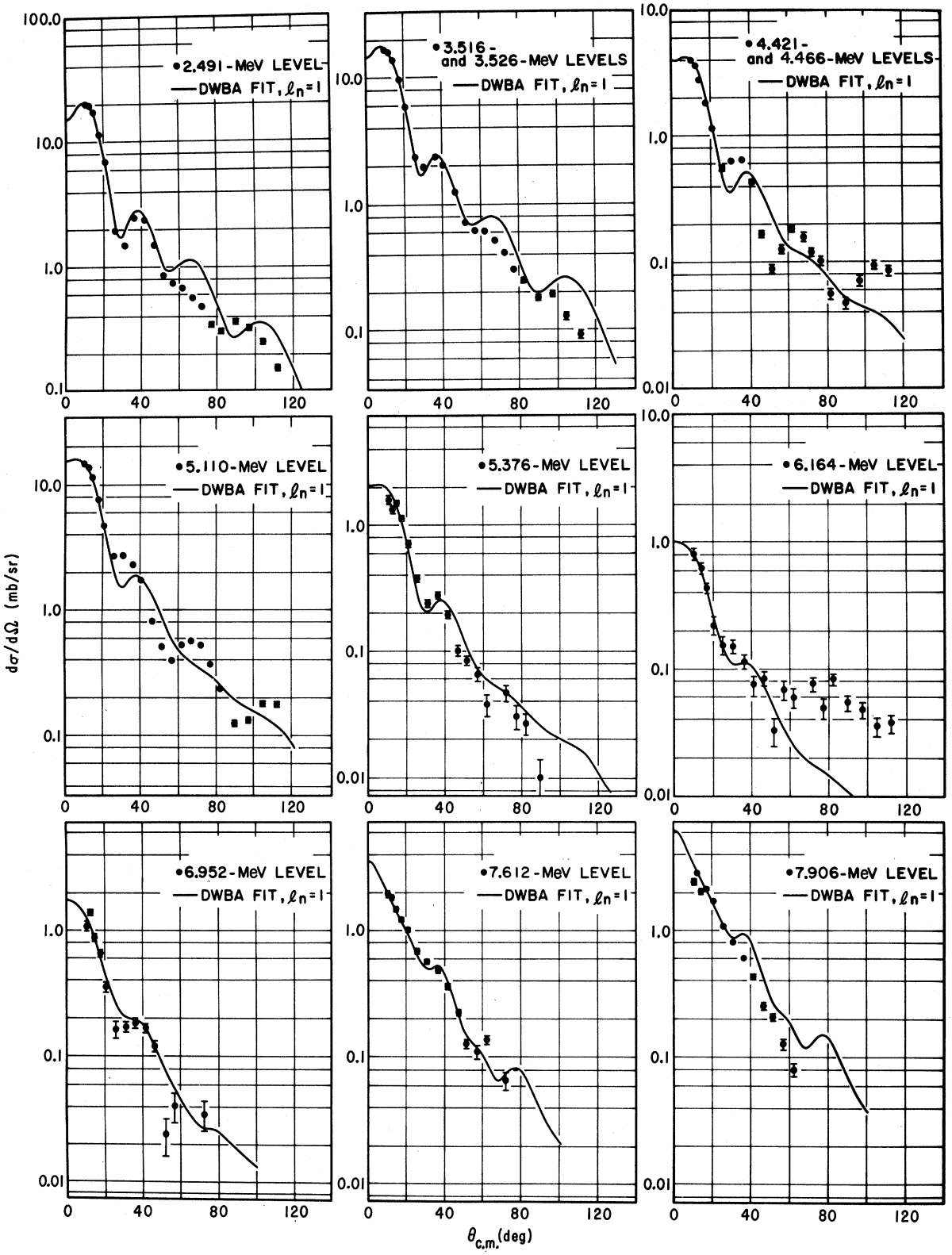

FIG. 15. $^{36}Ar(d,p)^{37}Ar$ angular distributions for nine groups which displayed $l=1$ character. The solid curves represent $l=1$, $2p$ DWBA fits for these (d,p) transitions as discussed in the text.

ment the (d, p) angular distributions were measured only out to $\simeq 90°$, and only out to $\simeq 40°$ for the case of $E_x > 5$-MeV levels in ^{33}S. At 18 MeV the transitions to the 4.935-MeV level in ^{29}Si and the 3.221- and 4.213-MeV levels in ^{33}S were the only $l_n = 1$ ^{28}Si(d, p) and ^{32}S(d, p) angular distributions analyzed out to at least 80°. All three are $\frac{3}{2}^-$ levels.[20] The shapes of these five $l_n = 1$ (d, p) angular distributions are essentially identical. However, the shapes of the $l_n = 1$ (d, p) angular distributions to the 4.466- and 5.110-MeV levels in ^{37}A are similar to one another but quite different from the five known $J = \frac{3}{2}$, $l_n = 1$ transitions (see Fig. 15). These two transitions have a minimum at $\simeq 54°$ with a secondary maximum at $\simeq 65°$, while the five (d, p) transitions to known $\frac{3}{2}^-$ levels show a monotonically decreasing cross section in this angular range. This is probably an $l_n = 1$ $(2p)$ J-dependent effect for the (d, p) reaction. The spins of the 4.466- and 5.110-MeV levels in ^{37}Ar have not been established by some independent experimental method, but spin assignments of $\frac{1}{2}^-$ to these levels are quite reasonable in a simple shell-model picture. Our 18.00-MeV results on the shapes of the strong $l_n = 1$ transitions in the ^{36}A(d, p) reaction are the same as those reported by Rosner and Schneid at 15.00 MeV.[8]

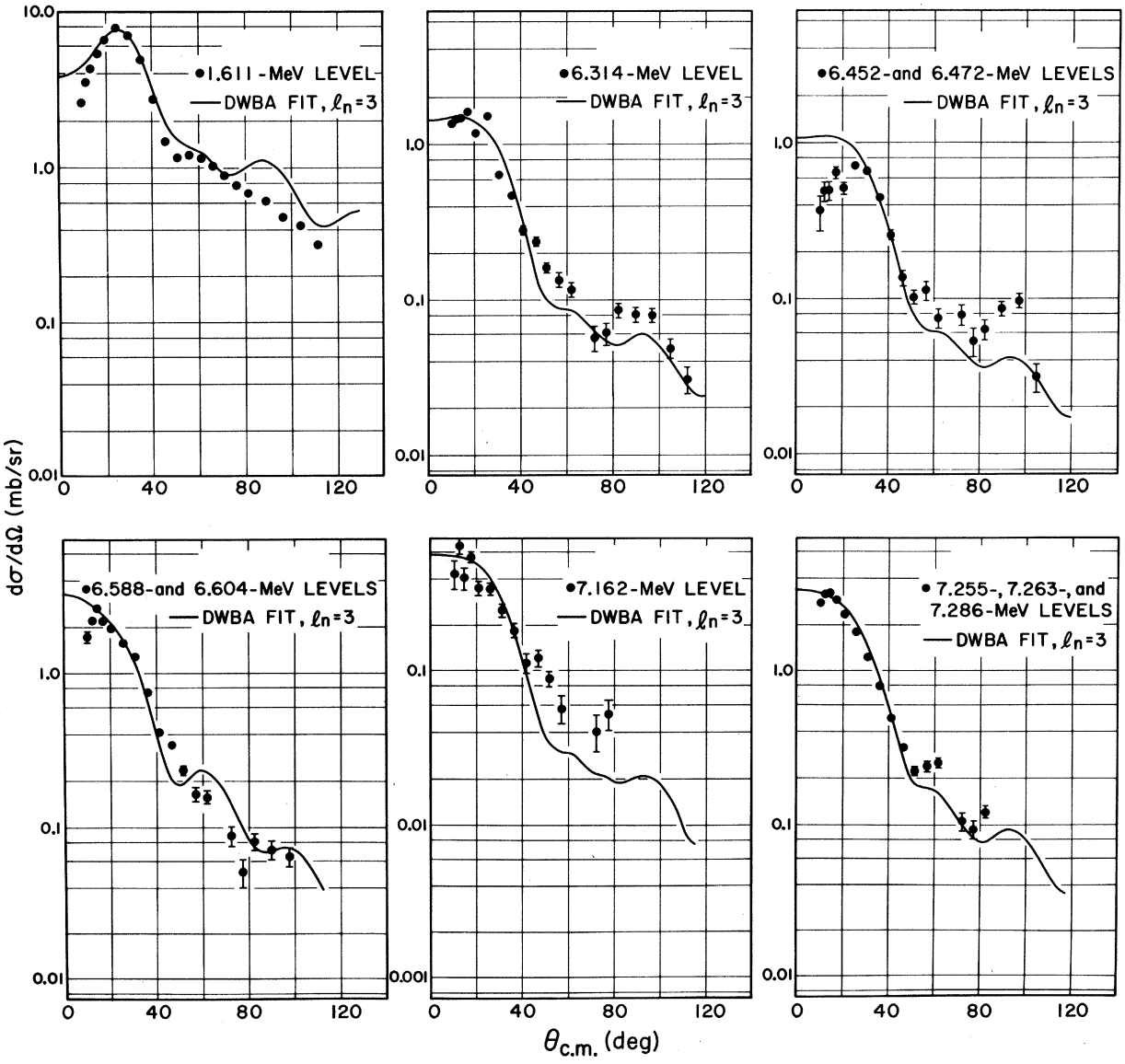

FIG. 16. ^{36}Ar$(d,p)^{37}$Ar angular distributions for six groups which displayed $l = 3$ character. The solid curves represent $l = 3$, $1f$ DWBA fits for these (d,p) transitions as discussed in the text.

V. COMPARISON WITH VARIOUS THEORETICAL MODELS

Table VII presents a comparison between the summed spectroscopic strengths, $\sum(2J+1)S$, measured in the present experiment for $2s$-$1d$, $1f$, and $2p$ (d, p) transfer on ^{28}Si, ^{32}S, and ^{36}Ar and the predictions of the simple shell model. In the simple shell model the $1f$ and $2p$ shells should be completely empty in these three nuclei, while the $2s$-$1d$ shell should have 20-N holes, where N is the neutron number of the target nucleus. The agreement, to within 25%, between experiment and the simple-shell-model picture for the summed $2s$-$1d$ spectroscopic strength in all three nuclei gives us considerable confidence in the basic accuracy of the DWBA analyses. Table VII indicates that the present experiment has located ~45% of the total $1f$ (d, p) spectroscopic strength in the ^{28}Si and ^{32}S (d, p) reactions, and ~65% of the total $1f$ strength in the ^{36}Ar(d, p) reaction. On the other hand, the present experiment seems to have located almost all of the total $2p$ spectroscopic strength in the ^{32}S(d, p) and ^{36}Ar(d, p) reactions (80 and 87%, respectively), and has located about 55% of the total $2p$ strength in the ^{28}Si(d, p) reaction. Part of the difference between these results for the $1f$ and $2p$ orbitals certainty lies in the greater sensitivity of the present experiment for $l_n = 1$, $2p$ (d, p) transfers. Some of the missing spectroscopic strength probably lies at higher excitation energies than those studied in the present experiment. SHR[23] report a fair amount of $l_n = 1$ $2p$ spectroscopic strength between excitation energies of 8.0 and 9.0 MeV in ^{37}Ar.

It is quite interesting to follow the general evolution of the spectroscopic factors for the negative-parity levels while the $2s$-$1d$ shell is being progressively filled in ^{29}Si, ^{33}S, and ^{37}Ar. In a regular fashion the excitation energy of the lowest $\frac{7}{2}^-$ level, which carries a large part of the total spectroscopic strength, decreases while its $l_n = 3$ $1f_{7/2}$ spectroscopic factor increases: $E_x(\frac{7}{2}^-\ ^{29}\text{Si}) = 3.623$ MeV, $S = 0.38$; $E_x(\frac{7}{2}^-\ ^{33}\text{S}) = 2.937$ MeV, $S = 0.57$; and $E_x(\frac{7}{2}^-\ ^{37}\text{Ar}) = 1.611$ MeV, $S = 0.77$. The excitation energy of the lowest $\frac{3}{2}^-$ level also decreases in a regular fashion, but its spectroscopic factor remains almost constant at 0.5 ± 0.1.

The present (d, p) neutron stripping experiment on ^{28}Si, ^{32}S, and ^{36}Ar, together with the previously reported (d, t) neutron-pickup experiments[2] on these same target nuclei, indicate no rapid change of nuclear shape as one moves from the nucleus with one neutron less to the nucleus with one neutron more than the target nucleus. If the nuclear shape were changing rapidly, one would expect unusually low cross sections for neutron-transfer reactions to the low-lying levels of the residual nuclei.[3, 26] However, for all three nuclei the $(d, t)^2$ and the present (d, p) reaction studies show large cross sections to the low-lying levels; and most of the total $2s$-$1d$ shell spectroscopic strength is represented by the transitions to the low-lying levels in the residual nuclei.

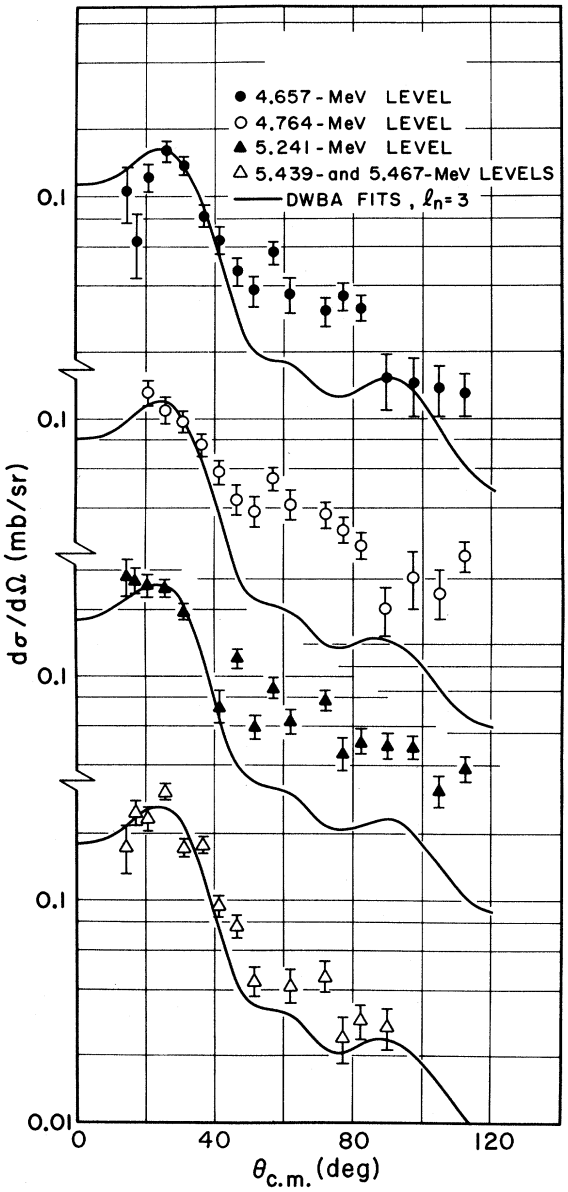

FIG. 17. ^{36}Ar$(d,p)^{37}$Ar angular distributions for four relatively weak groups which displayed behavior suggestive of $l = 3$ transfer. The solid curves represent $l = 3$, $1f_{5/2}$ DWBA fits to these (d,p) transitions. As discussed in the text, transitions identified with the formation of these same levels appear much more intense and display $l = 1$ transfer character in a similar experiment carried out at $E_d = 9.162$ MeV (Ref. 23).

Within the context of the strong-coupling model with no band mixing, the spectroscopic factor, $S_{j\alpha}$, for the excitation of a particular level by the (d, p) reaction on a zero-spin target nucleus may be expressed as[27]

$$S_{j\alpha} = \frac{2(C_{j\alpha})^2}{2j+1} \langle \phi_f | \phi_f \rangle^2 . \quad (1)$$

Here j is the spin of the stripped neutron and the spin of the residual nuclear state, $C_{j\alpha}$ is the Nilsson coefficient of the deformed orbit α, and $\langle \phi_f | \phi_i \rangle$ is the core overlap, which is usually assumed to be one. Since the $C_{j\alpha}$ are less than or equal to 1, Eq. (1) leads directly to an upper limit on the spectroscopic factor $S_{j\alpha}$:

$$S_{j\alpha} \leq 2/(2j+1) . \quad (2)$$

The upper limit represented by Eq. (2) is exceeded by many (d, p) transitions measured in the present experiment. For example, the experimental spectroscopic factors for the excitation of the $\frac{3}{2}^+$ 1.273-MeV ^{29}Si level and the $\frac{3}{2}^+$ ^{37}Ar ground state are 0.74 and 0.93, respectively, while Eq. (2) predicts $s_{3/2\alpha} \leq 0.50$. Also, the lowest-lying $\frac{7}{2}^-$ levels in ^{29}Si, ^{33}S, and ^{37}Ar all have spectroscopic factors which are much larger than the maximum value of 0.25 predicted by Eq. (2).

The (d, p) spectroscopic factors measured in the present experiment may also be compared with those predicted by the Hartree-Fock calculations of Ripka,[28] Bar-Touv and Kelson,[29] and Bar-Touv *et al.*[30] The general agreement is quite poor; and this disagreement has been discussed by Ripka.[26] In particular it is difficult to reconcile the Hartree-Fock calculations with the experimental (d, p) spectroscopic factor for the $\frac{1}{2}^+$ 0.842-MeV level in ^{33}S. All the Hartree-Fock calculations[28-30] would give this level a spectroscopic factor on the order of 0.01, while the experimental value is 0.32. Thus the present experiment would seem to rule against the picture that the nuclear structure in the upper half of the $2s$-$1d$ shell can be explained in terms of unmixed rotational bands based on deformed-orbital Hartree-Fock calculations. This result is in agreement with our previous (d, d') inelastic scattering analyses[1] on ^{28}Si, ^{32}S, and ^{36}Ar where it was concluded that ^{28}Si most probably has an oblate equilibrium shape while ^{32}S and ^{36}Ar most probably have spherical equilibrium shapes. It is interesting to note that recent calculations[31,32] which include the effects of two-particle–two-hole admixtures on the Hartree-Fock field have indicated a spherical shape for the ^{32}S ground state.

A group at the Oak Ridge National Laboratory has recently made available an extensive set of shell-model calculations in the $2s$-$1d$ shell. This work has been summarized in two articles.[4,33] These shell-model calculations predict wave functions, excitation energies, and one-nucleon-transfer spectroscopic factors, so that a direct comparison can be made with the present (d, p) experimental studies. In the mass region $A = 30$ to 33, the Oak Ridge calculations use a truncated shell-model basis which includes all possible $2s_{1/2}$ and $1d_{3/2}$ configurations with no more than two holes being allowed in the $1d_{5/2}$ shell – in the simplest shell-model picture the $1d_{5/2}$ shell would be filled

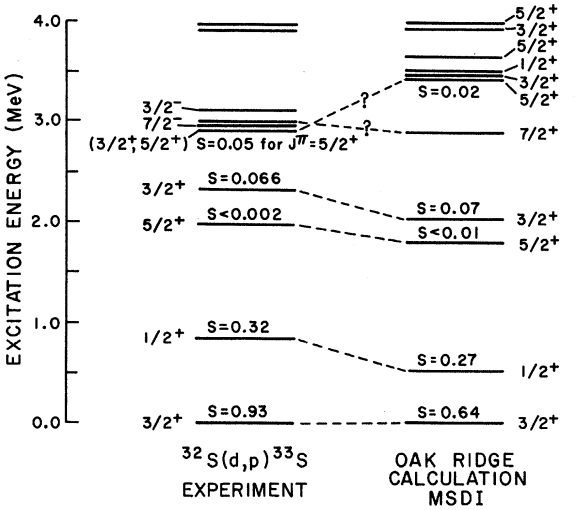

FIG. 18. Comparison of the experimental ^{32}S(d,p) spectroscopic factors for the positive-parity states of ^{33}S and the predictions of the Oak Ridge shell-model calculations (Ref. 35) which use a modified surface δ interaction (MSDI) as the effective interaction.

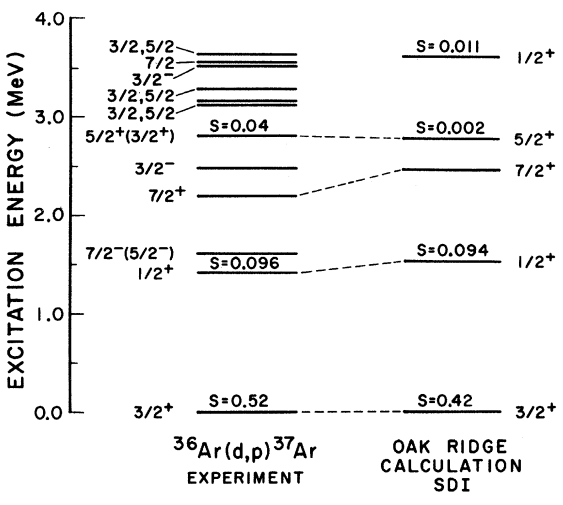

FIG. 19. Comparison of the experimental ^{36}Ar(d,p) spectroscopic factors for the positive-parity states of ^{37}Ar and the predictions of the Oak Ridge shell-model calculations (Ref. 35) which use a surface δ interaction (SDI) as the effective interaction.

at ^{28}Si. In the mass region $A = 34$ to 39, these calculations use the complete basis of all possible $1d_{5/2}$, $2s_{1/2}$, and $1d_{3/2}$ configurations. Unfortunately no calculations are available for $A = 29$, since the region near the middle of a shell produces the largest number of possible configurations; and truncation of the shell-model basis is difficult to justify. Thus there are no Oak Ridge calculations to compare with our ^{28}Si(d, p) experimental results.

Figures 18 and 19 compare the present experimental results with the Oak Ridge predictions for the reactions ^{32}S$(d, p)^{33}$S and ^{36}Ar$(d, p)^{37}$Ar, respectively. The Oak Ridge calculations predict only positive-parity levels based on $2s$-$1d$ configurations. The agreement between experiment and theory is quite good. The calculations in Fig. 18 used a modified surface δ interaction (MSDI) as the effective interaction.[34] The Oak Ridge group has previously compared our ^{32}S$(d, p)^{33}$S experimental results with their calculations.[35] It should be mentioned that an earlier calculation by Glaudemans, Wieckers, and Brussaard,[36] which used a $2s_{1/2}$-$1d_{3/2}$ shell-model basis with a filled $1d_{5/2}$ shell at ^{28}Si, is also in reasonable agreement with the present ^{32}S$(d, p)^{33}$S results, as regards to the $2s_{1/2}$ and $1d_{3/2}$ (d, p) transitions. The Oak Ridge calculations presented in Fig. 19 used a surface δ interaction (SDI) as the effective interaction. Other choices for the effective interaction have been made by the Oak Ridge group,[4] but the (d, p) spectroscopic factors do not appear to be too sensitive to the exact choice of the effective interaction.

In summary, as was the case with the previously reported (d, t) reaction studies on ^{32}S and ^{36}Ar,[2] quite good agreement has been found between the present ^{32}S(d, p) and ^{36}Ar(d, p) experimental studies and the Oak Ridge shell-model calculations with regard to the positive-parity $2s$-$1d$ nuclear states. It is hoped that the present body of (d, p) experimental data on ^{28}Si, ^{32}S, and ^{36}Ar, as well as the previously reported (d, t) and (d, d') reaction studies[1,2] on these same three nuclei will stimulate further theoretical study of the upper s-d nuclei.

ACKNOWLEDGMENTS

We are indebted to Kenzo Sato and the operating staff of the A. W. Wright Nuclear Laboratory for their assistance during these experiments. It is a pleasure to thank again Dr. George Ripka for having stimulated this experimental work and for his enlightening discussions. We would also like to thank the Oak Ridge Theoretical Group of Dr. P. W. M. Glaudemans, Dr. E. Halbert, Dr. J. B. McGrory, and Dr. B. H. Wildenthal for providing us with their recent $2s$-$1d$ shell calculations. One of the authors (CAW) would like to thank Dr. H. J. Young for providing some valuable unpublished data and the Physics Department at the University of California at Los Angeles for providing secretarial help in the preparation of this manuscript.

---

*Work supported in part by the U. S. Atomic Energy Commission under Contract No. AT(30-1)3223.

† NATO Fellow on leave of absence from the Center of Nuclear Research, Saclay, France. Present address: Center of Nuclear Research, Saclay, France.

‡ Present address: Physics Department, University of California at Los Angeles, Los Angeles, California 90024.

§ Permanent address: Trinity College, Hartford, Connecticut 06106.

[1] M. C. Mermaz, C. A. Whitten, Jr., and D. A. Bromley, Phys. Rev. 187, 1466 (1969).

[2] C. A. Whitten, Jr., M. C. Mermaz, and D. A. Bromley, Phys. Rev. C 1, 1455 (1970).

[3] G. Ripka, in *Proceedings of the International Nuclear Physics Conference, Gatlinberg, Tennessee, September 1966,* edited by R. L. Becker and A. Zucker (Academic, New York, 1967), p. 833.

[4] E. Halbert, in *Proceedings of the Third International Conference on the Structure of Low-Medium Mass Nuclei, University of Kansas, 1968,* edited by J. P. Davidson (University Press of Kansas, Lawrence, Kansas, 1968).

[5] P. M.Endt and C. Van der Leun, Nucl. Phys. A105, 1 (1967), and the references therein.

[6] A. G. Blair and K. S. Quisenberry, Phys. Rev. 122, 869 (1961).

[7] M. Betigeri, R. Bock, H. H. Duhm, S. Martin, and R. Stock, Z. Naturforsch. 21a, 980 (1966).

[8] B. Rosner and E. J. Schneid, Phys. Rev. 139, B66 (1965).

[9] F. S. Goulding, D. A. Landis, J. Cerny, and R. J. Pehl, Nucl. Instr. Methods 31, 1 (1964).

[10] The system was fabricated in this laboratory by C. E. L. Gingell and his staff.

[11] Hamilton Watch Company, Lancaster, Pennsylvania.

[12] E. A. Silverstein, Nucl. Instr. Methods 4, 53 (1959).

[13] R. H. Bassel, R. M. Drisko, and G. R. Satchler, Oak Ridge National Laboratory Report No. ORNL-3240 and Suppl., 1962 (unpublished).

[14] G. R. Satchler, Nucl. Phys. 55, 1 (1964).

[15] F. G. Perey, Phys. Rev. 131, 745 (1963).

[16] L. J. B. Goldfarb, Phys. Letters 24B, 264 (1967).

[17] J. P. Schiffer, L. L. Lee, Jr., A. Marinov, and C. Mayer-Böricke, Phys. Rev. 147, 829 (1966).

[18] J. Kopecky and E. Warming, Nucl. Phys. A127, 385 (1969).

[19] H. J. Young, R. L. Becker, and W. H. Moore, Bull. Am. Phys. Soc. 15, 484 (1970); and H. J. Young, private communication.

[20] J. W. Champlin, A. J. Howard, and J. W. Olness, Nucl. Phys. A164, 307 (1971).

[21] C. H. Holbrow, P. V. Hewka, J. Wiza, and R. Middle-

ton, Nucl. Phys. 79, 505 (1966).
[22]E. Kashy, A. M. Hoogenboom, and W. W. Buechner, Phys. Rev. 124, 1917 (1961).
[23]S. Sen, C. L. Hollas, and P. J. Riley, Phys. Rev. C 3, 2314 (1971).
[24]W. Fitz, R. Jahr, and R. Santo, Nucl. Phys. A114, 392 (1968).
[25]L. L. Lee, Jr., and J. P. Schiffer, Phys. Rev. 136, B405 (1964).
[26]G. Ripka, in *Proceedings of the Third International Conference on the Structure of Low-Medium Mass Nuclei, University of Kansas, 1968*, edited by R. L. Becker and J. P. Davidson (University Press of Kansas, Lawrence, Kansas, 1968).
[27]G. R. Satchler, Ann. Phys. (N.Y.) 3, 275 (1958).
[28]G. Ripka, in *Advances in Nuclear Physics*, edited by M. Baranger and E. Vogt (Plenum, New York, 1968), Vol. 1.
[29]J. Bar-Tuov and I. Kelson, Phys. Rev. 138, B1035 (1965).
[30]J. Bar-Tuov, A. Goswami, A. L. Goodman, and G. L. Struble, Phys. Rev. 178, 1670 (1969).
[31]R. Padjen and G. Ripka, Phys. Letters 29B, 548 (1969).
[32]R. Padjen and G. Ripka, Nucl. Phys. A149, 273 (1970).
[33]J. B. French, E. C. Halbert, J. B. McGrory, and S. S. Wong, in *Advances in Nuclear Physics*, edited by M. Baranger and E. Vogt (Plenum, New York, 1969), Vol. 3.
[34]P. W. M. Glaudemans, P. J. Brussaard, and B. H. Wildenthal, Nucl. Phys. A102, 593 (1967).
[35]B. H. Wildenthal, J. B. McGrory, and E. C. Halbert, Phys. Letters 27B, 611 (1968).
[36]P. W. M. Glaudemans, G. Wiechers, and P. J. Brussaard, Nucl. Phys. 56, 548 (1964).

PHYSICAL REVIEW C VOLUME 4, NUMBER 5 NOVEMBER 1971

Masses and Half-Lives of ^{20}Na, ^{24}Al, ^{28}P, ^{32}Cl, and ^{36}K from the (p,n) Reaction*

D. R. Goosman, K. W. Jones, E. K. Warburton, and D. E. Alburger
Brookhaven National Laboratory, Upton, New York 11973
(Received 17 June 1971; revised manuscript received 15 September 1971)

The (p,n) thresholds for the formation of ^{20}Na, ^{28}P, ^{32}Cl, and ^{36}K from targets of ^{20}Ne, ^{28}Si, ^{32}S, and ^{36}Ar, respectively, have been measured relative to the ^{24}Mg$(p,n)^{24}$Al threshold by detecting β rays from these short-lived activities. Half-lives were determined by multiscaling techniques. The resulting (p,n) thresholds (in keV), half-lives (in msec) are as follows: ^{20}Na (15 419 ± 6, 442 ± 5); ^{28}P (15 666 ± 6, 266 ± 4); ^{32}Cl (13 902 ± 9 and 13 978 ± 16, 281 ± 8); ^{36}K (13 976 ± 8, 336 ± 4). The half-life of ^{24}Al was measured as 2.054 ± 0.009 sec.

I. INTRODUCTION

In a recent series of reports[1-5] Wilkinson and Alburger have instituted a careful study of mirror symmetry in β decay. The point of view of this series was the possible existence of second-class terms[6] in the β-decay operator. From the most recent work in their series, a study of the mass-8 system,[5] it appears that the bulk of the deviation from mirror symmetry of β decay is not due to second-class terms but to nuclear-structure effects larger than heretofore expected, or to some so-far-unforeseen effect. This becomes a question of theoretical interest. Regardless of the outcome of this question, it has been reemphasized by this work that the comparison of mirror β decays is a fruitful way of testing our knowledge of the nucleus, and it is clear that our understanding should be good enough to demand as accurate a comparison as present experimental techniques allow.

The desire for more accuracy was, then, the main motive for initiating the studies of the $(p, n\beta^+)$ reactions reported herein. The targets used were the $4n$, $T_z = 0$ nuclei from ^{20}Ne to ^{36}Ar. Measurements consisted of (p,n) threshold determinations and therefore masses for ^{20}Na, ^{28}P, ^{32}Cl, ^{32}Cl*, and ^{36}K all relative to the mass of ^{24}Al, and half-life determinations for the positron emitters ^{20}Na, ^{24}Al, ^{28}P, ^{32}Cl, and ^{36}K. The results for ^{20}Na have been briefly reported previously[4]; they are included here for completeness.

II. EXPERIMENTAL METHODS AND RESULTS

The five (p,n) reactions under study have thresholds in the proton energy range from 13.9 to 15.7 MeV. Proton beams of the desired energy were provided by the second tandem of the Brookhaven National Laboratory three-stage MP tandem Van de Graaff facility. The thresholds for the various (p,n) reactions, and the half-lives of the activities produced were measured by detecting the emitted β rays in a 5-cm-diam × 2.5-cm-thick NE 102 plastic scintillator attached to an RCA 6342 photomulti-